Original Research Article

Characterisation of the Vertical Wind Profile According to the Stability Classes of the Atmosphere in Conakry, Guinea

ABSTRACT

The characteristics of the vertical wind profile and the wind potential study on the Conakry site for each atmospheric stability class were investigated in this study. Wind speed and air temperature data recorded over the period from January 2001 to December 2019 at 10 m and 50 m above the ground at daily (50 m) and hourly (10 m) scales were used. The wind shear parameters were determined from the logarithmic and power law. Based on the Newman and Klein wind shear model, a new formulation of this parameter was proposed as a function of the Obukhov length at order 2 and calibrated from the measurements using the simplex algorithm of Nelder and Mead. From the Weibull parameters obtained for the stable and unstable period of the atmosphere, the available wind potential at Conakry was estimated from 10 m to 80 m. The results indicate that the annual average of the ground roughness length is 1.7 x 10^{-2} m. The annual average of the ground friction velocity is 0.19 $m.s^{-1}$. The atmosphere remains stable at the Conakry site from 09 p.m. to 10 a.m. and unstable from 10 a.m. to 09 p.m. The proposed wind shear formulation gives a better estimation of the wind speed in function of altitude with the lowest values of RMSE and MAE ($4.5x10^{-4}$; $3.8x10^{-4}$) $m.s^{-1}$ in stable and unstable periods (0.09 ; 0.07) $m.s^{-1}$ compared to some models found in the literature. The mean annual wind shear coefficient in stable period is 0.26 and in unstable period 0.28. The annual mean shape parameter from 10 m to 80 m above ground in stable period is between 1.25 and 1.64, and during unstable period, it varies from 1.55 to 2.07. The annual mean scale parameter at 10 m and 80 m above ground is (3.9 ; 7.10) $m.s^{-1}$ (unstable atmosphere) and (2.45 ; 4.41) $m.s^{-1}$ when the atmosphere is stable. The annual average of the energy production under a convective atmosphere at 10 m and 80 m is estimated at 72 $W.m^{-2}$ and 301 $W.m^{-2}$ respectively. During the night cycle, this annual production varies from 28 $W.m^{-2}$ (10 m) to 93 $W.m^{-2}$ (80m). Based on these results, the Conakry site is suitable to host medium-sized wind power plants for electricity and water production.

Keywords: Wind profile; Atmospheric stability; Theory of Monin-Obukov; Power law; Wind energy

ABBREVIATIONS

V_h : the wind speed at altitude Z_h ($m.s^{-1}$)
V_1 : the wind speed at 10 m ($m.s^{-1}$)
Z_0: the roughness length (m)
u_*: the speed of friction ($m.s^{-1}$)
$\overline{v}$: wind average speed ($m.s^{-1}$)
V_{mp} :the most probable ($m.s^{-1}$)
V_{Emax}: maximum energy carrying wind speeds ($m.s^{-1}$)
T: the temperature of air (°K)

T_0 : the average temperature (°K)
U : the hourly horizontal wind speed at 10 m ($m.s^{-1}$)
P : the wind power ($W.m^{-2}$)
ρ : the air density at the site ($Kg.m^{-3}$)
g : the gravity ($m^2.s^{-1}$)
L : Obukhov length (m)
Z_1 : the height at 10 m (m)
$\sigma^2(T)$: the variance of the air temperature(°K)
$\sigma^2(w)$: the variance of the vertical wind component ($m.s^{-1}$)
c : the scale parameter ($m.s^{-1}$)
Γ : gamma function
κ : the von Karman constant
α : wind shear coefficient
R_i is Richardson number
a : fitting constants
b : fitting constants
c : fitting constants
d : fitting constants
$\Psi_m\left(\frac{Z_h}{L}\right)$: the universal stability function
pi : represents the observations
fi the different estimates or predictions
N : the total number of wind speed observations
k : the Weibull shape parameter
$\overline{w'T'}$: the heat flux density
$f(v)$: the probability of observing wind speed
Fig: Figure

1. INTRODUCTION

The advent of climate change and the depletion of fossil resources have raised international awareness of the need to explore other sources of energy, particularly green energy. Among these sources, wind energy has been widely exploited in the world during the last two decades [1]. In wind energy systems, wind speed plays the most important role in the assessing of the available wind resource. Therefore, during the feasibility study phase for the implementation of wind farms, the use of wind data is an essential step to better assess the quality and quantity of energy that can be expected at the hub height of the wind turbines [2]. Unfortunately, very little wind data is available at altitudes above 10 m. Those that are generally known require the installation of large towers or more expensive devices such as LIDAR or SODAR to perform the measurements [3]. These measurement methods increase the cost of wind energy projects, often making them economically not viable [4]. It is therefore of utmost importance to develop reliable techniques to determine the vertical wind profile at the desired height for the siting of a wind turbine in order to address these wind data deficiencies. This motivation has been mentioned by several authors such as [5-7] who endorse wind shear characterisation. Among the wind extrapolation methods, the power law and the logarithmic law are commonly used and developed by many authors such as [2,8-22]. However, some of these authors do not taking into account atmospheric stability and ground topography, which play an important role in the formation of wind speed profiles [2]. Moreover, there is not yet a fast, reliable and universal model to better estimate the wind speed at any site [3] because of the specificities of each region. Poje and Cividini [23] therefore propose as preferable solutions, which will be the subject of this study, to establish a specific model for each site considered from the available data.

The establishment of this model for Conakry was based on the power law method, which is a function of the atmosphere stability and was also developed by Xu et al [2] in order to produce the most suitable model for the study site. The method uses the estimated wind shear exponent under different stability conditions rather than its average value under all stability conditions. According to the work of Mathos et al [24], the Conakry site was found to be one of the windiest in Guinea. This site was therefore chosen as the study environment. The wind data available at this site are hourly at 10 m and daily at 50 m above the ground. To approach this study in a first step, the wind shear parameters (roughness length, friction speed, shear coefficient) were determined for the site of Conakry using the power law and logarithmic from the daily averages at 10 m and 50 m above the ground. In a second step, from hourly temperature and wind speed data at 10 m, the stability classes of the atmosphere were characterized by determining the Obukhov length. The vertical wind speed profile for each stability class of the atmosphere was then estimated using the Monin-Obukhov theory as a function of roughness and Obukhov length. A new formulation of the wind shear coefficient was proposed for the Conakry site using the Newman and Klein model. The calibration of the proposed model was performed using the Nelder-Mead algorithm. Finally, the wind energy potential of the site for the stable and unstable period of the atmosphere was determined between 10 m and 80 m above the ground. In this study the neutral stability class was not addressed.

2. MATERIAL AND METHODS

2. 1 Material

2.1.1 Presentation of the study area

Conakry, located on the Atlantic Ocean, is the capital and largest city of Guinea. It extends between 9°35 and 9°40 (north latitude) and 13°37 and 13°42 (West longitude). With a surface area of 450 km² and a density of 5150 inhabitants/km², Conakry has 2,317,376 inhabitants**.** Located in the southwest of Guinea, on the Camayenne peninsula, near the Loos Islands, the city of Conakry extends over the coastal plain crossed by small rivers that flow down from Fouta-Djalon. The territory of the city is oriented north-east/south-west and ends with the peninsula of Kaloum and the island of Tombo. Conakry enjoys a tropical climate. The dry season (November to mid-May) is under the influence of the harmattan. The rainy season is intense and reminding the monsoon. The minimum temperatures are between 22°C and 24°C**. The** maximum temperatures vary between 28°C and 31°C**.** Figure 1 provides an overview of the Conakry site.

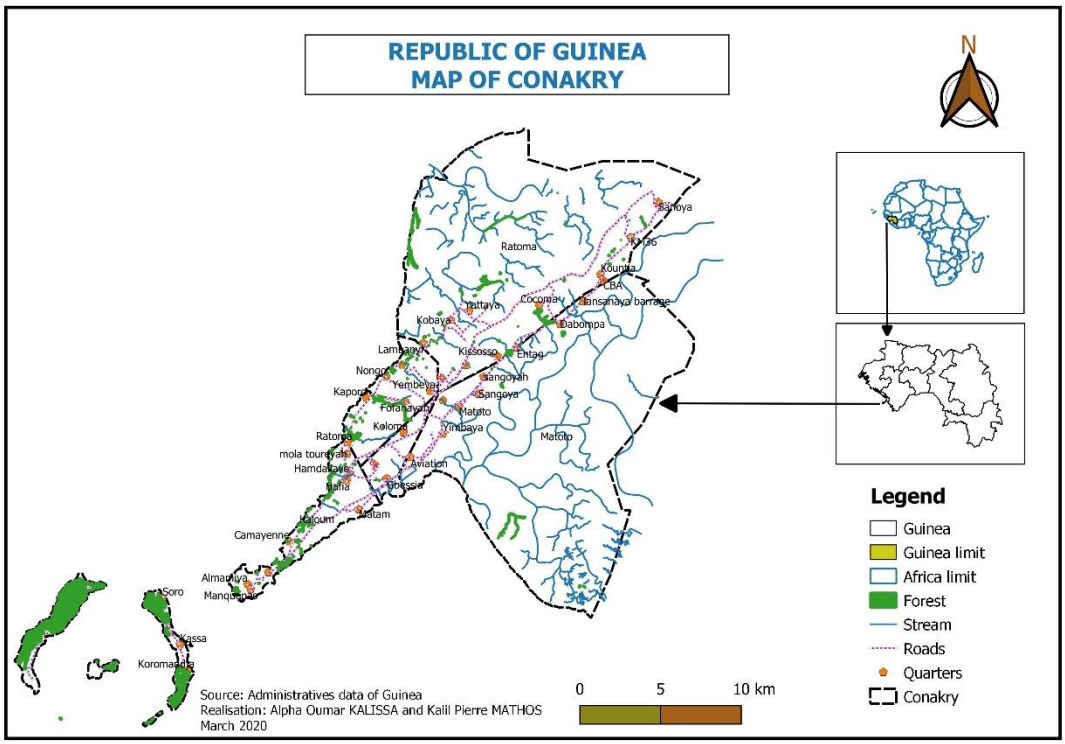

Fig.1. Map of the study area

The geographical characteristics of the Conakry site are presented in Table 1.

Table 1 Geographical characteristics of the measurement site

Site	Longitude	Latitude	Height
Conakry	13°34’ O	9° 34’ N	**10 m**

2.1.2 Data used

The data used is composed of wind speed and ambient air temperature series recorded on an hourly and daily scale during the period from January 2001 to December 2019. The wind and temperature data of the Ambient air collected respectively at 10 m and 2 m above the ground at the scale of one hour are ERA 5 reanalyses. These series constitute a mixture of real data and model data merged over a period of 40 to 50 years approximately. The principle of reanalysis for phenomena is based on the recomposition of the parameter studied by the IFS (Integrated Forecasting System) model of the European Center for Medium-Range Weather Forecasting (ECPMMT). The daily wind speeds recorded at 10 m and 50 m above the ground are provided by the Guinean National Meteorological Department and NASA. Daily average wind speeds include minimum, maximum and average wind speed.

2.2. Methods

2.2.1 Vertical wind profile modeling

2.2.1.1 The power law

The power law is a method which allows to estimate the wind speed at a desired altitude in the surface boundary layer from the known wind speed at a lower altitude. This technique is simpler to use and that is why, in the work carried out by Justus and Mikhail [8], the authors preferred adopt it. It was proposed by Hellman [25] and used in several works such as [2, 3, 18, 12, 26-27]. To model the wind profile according to the stability classes of the atmosphere in Conakry, the power law was used.

$$\frac{V_h}{V_1} = \left(\frac{Z_h}{Z_1}\right)^{\alpha} \quad (1)$$

where V_1 is the wind speed at altitude Z_1 equal to 10m, V_h is the wind speed at altitude Z_h. This law is a function only of the wind shear coefficient α. Its value depends on several factors such as atmospheric stability, the characteristics of the ground (topography and roughness Z_0 [28, 29]). From equation (1), the coefficient α is determined by :

$$\alpha = \frac{\ln(V_h) - \ln(V_1)}{\ln(Z_h) - \ln(Z_1)} \quad (2)$$

2.2.1.2 Estimation of roughness and ground friction velocity

Roughness is the height of asperities that can be encountered on a surface. On a site it represents the aerodynamic effects of the topographic elements in the surface layer. As for the friction velocity, it provides information on the intensity of the turbulent movement of air masses on the ground surface due to the asperities present. Considering the logarithmic law, these two parameters are determined from a logarithmic least squares regression after a change of variable. The logarithmic law is given by :

$$V_h = \left(\frac{u_*}{\kappa}\right)\left[\ln\left(\frac{Z_h}{Z_0}\right)\right] \quad (3)$$

With Z_0 the roughness length (m), u_* the speed of friction ($m.s^{-1}$) and κ the von Karman constant equal to 0.4. Transforming equation (3) by the properties of logarithms, equation (3) becomes by a change of variable :

$$V_h = X \ln(Z_h) + Y \quad (4)$$

With

$$X = \left(\frac{u_*}{\kappa}\right) \quad (5)$$

$$Y = -\left(\frac{u_*}{\kappa}\right) \ln(Z_0) \quad (6)$$

Knowing therefore X and Y by logarithmic least squares regression the roughness and the friction velocity will be deduced. The friction velocity, roughness and wind shear coefficient were determined from the daily wind speed data at 10 m and 50 m above the ground.

2.2.1.3. Stability class of the atmosphere

To determine the stability classes of the atmosphere, several methods exist and are used. The one chosen in this study according to the available data is the Monin-Obukhov method. The Obukhov length which allows to determine the different classes of stability of the atmosphere is given by :

$$L = \frac{-u_*^3 T_0}{\kappa g \overline{w'T'}} \quad (7)$$

Or $\overline{w'T'}$ represents the heat flux density and is also equal to the covariance of the vertical wind component and the temperature T of the ambient air $\left(\overline{w'T'} = \mathrm{cov}(w,T)\right)$, w is the vertical component of the wind at 10 m above the ground, g is the gravity, and T_0 is the average temperature.
The $\mathrm{cov}(w,T)$ has been computed from the Cauchy Schwarz inequality which is based on the mathematical properties of covariance. Thus, we have [3]:

$$[\mathrm{cov}(w,T)]^2 \leq \sigma^2(w)\sigma^2(T) \quad (8)$$

Or $\sigma^2(T)$ and $\sigma^2(w)$ are the variance of the air temperature and the variance of the vertical wind component.
The standard deviation of the vertical wind component can be expressed from the standard deviation of the horizontal wind speed U by [3, 30] :

$$\sigma_w = 0{,}45\sigma_U \quad (9)$$

U is the hourly horizontal wind speed at 10m above the ground.

The Obukhov length was determined from hourly wind speed and air temperature data at 10 m. The different classes of atmospheric stability as a function of Obukhov length are summarized in Table 2.

Table 2 Atmospheric stability classes according to the Obukhov length [3, 31]

Stability class	Obukhov length [m]
Very stable	$0 \prec L \prec 200$
Stable	$200 \prec L \prec 1000$
Neutral	$\lvert L \rvert \succ 1000$
Unstable	$-200 \prec L \prec 0$
Very unstable	$-1000 \prec L \prec -200$

2.2.1.4. Estimation of the vertical wind profile as a function of atmospheric stability

To characterize the vertical wind profile in Conakry, the average wind speeds at 10 m from the ground for the stable and unstable period were calculated. Indeed, after having determined the stability classes of the atmosphere obtained from the Obukhov length, the hourly wind speeds were separated into stable and unstable periods and the averages were then determined for each stability period. Since hourly wind and temperature data at 50 m above ground level were not available, we opted for the Monin and Obukhov model [32], which is a function of atmospheric stability, to estimate wind speed at altitudes greater than

10 m from the average speeds for each stability period calculated previously. It is given by equation (10):

$$V_h = V_1 \left[\frac{\ln\left(\frac{Z_h}{Z_0}\right) - \Psi_m\left(\frac{Z_h}{L}\right)}{\ln\left(\frac{Z_1}{Z_0}\right) - \Psi_m\left(\frac{Z_1}{L}\right)} \right] \quad (10)$$

$\Psi_m\left(\frac{Z_h}{L}\right)$ is the universal stability function, Z_1 is the height at 10 m. According to the studies of Paulson [33] reported by Businger [34], we have the following equation for an unstable atmospheric condition $\left(\frac{Z_h}{L} < 0\right)$:

$$\Psi_m\left(\frac{Z_h}{L}\right) = 2\ln\left(\frac{1+x}{2}\right) + \ln\left(\frac{1+x^2}{2}\right) - 2\tan^{-1}(x) + \frac{\pi}{2} \quad (11)$$

With :

$$x = \left(1 - 16\frac{Z_h}{L}\right)^{\frac{1}{4}} \quad (12)$$

For stable conditions the power law was used with the shear model proposed by Panosfky and Dutton [35] :

$$\alpha = \frac{\left(1+\frac{5Z}{L}\right)}{\ln\left(\frac{Z}{Z_0}\right)+\left(\frac{Z}{L}\right)} \quad (13)$$

Once the average wind profile was determined for each class of the atmosphere stability, we used the wind shear model proposed by Newman and Klein [18] to characterize this profile at the Conakry site. Indeed, in this work, Newman and Klein [18] have developed wind shear equations from the following formulation for stable and unstable conditions of the atmosphere:

$$\alpha = \alpha_0(1 + aR_i)^b \quad (14)$$

R_i is Richardson number, a and b are the constants. Based on this equation (14), we propose a new formulation of the wind shear at the Conakry site by modifying the formulation of Newman and Klein [18]. It is expressed as a function of the Obukhov length at order 2. The coefficient α is as follows :

$$\alpha = \alpha_0(1 + cL + aL^2)^b \quad (15)$$

where the values of a and b were determined separately for stable and unstable regimes of the atmosphere using the local numerical optimization method based on the simplex algorithm of Nelder and Mead [36] reported by Lagarias et al [37]. This algorithm is one of the most widely adopted methods for unconstrained nonlinear multidimensional optimization and was used in this study to better calibrate the proposed wind shear coefficient in equation (15) with measurements. In Matlab software, the function fminsearch was used to simulate this algorithm. Fminsearch finds the minimum of a scalar function of several variables, starting with an initial estimate. α_0 is given by Spera and Richards [38]:

$$\alpha_0=\left(\frac{z_0}{z_1}\right)^d \quad (16)$$

2.2.1.5 Error estimation test

The root mean square error (RMSE) measures the average magnitude of errors made by the prediction. It is one of the most widely used indicators of the error between measurements and estimations. It is given by [39,41] :

$$\mathrm{RMSE}=\sqrt{\frac{1}{N}\sum_{i=1}^{n}(P_i-f_i)^2} \quad (17)$$

where pi represents the observations, fi the different estimates or predictions, and N the total number of wind speed observations. When its value is small and close to zero the estimator is better. The mean absolute error test has also been calculated. It is given by [41, 42] :

$$\mathrm{MAE}=\frac{1}{N}\sum_{i=1}^{n}\left|P_i-f_i\right| \quad (18)$$

2.2.2 Wind energy modeling

2.2.2.1 Wind speed distribution

The wind speed distribution used to represent the occurrence frequencies in a suitable way is the Weibull distribution [43-45]. This distribution has therefore been used and it expresses as follows [46-51]:

$$f(v)=\left(\frac{k}{c}\right)\left(\frac{v}{c}\right)^{k-1}\exp\left[-\left(\frac{v}{c}\right)^{k}\right] \qquad k>0, v>0, c>0 \quad (19)$$

where k is the Weibull shape parameter, c is the scale parameter, v is the wind speed and f(v) is the probability of observing wind speed. To calculate the shape parameter k, the method used in this study is given by the following approximation [51, 52]:

$$k=0.83(\overline{v})^{0.5} \quad (20)$$

The scale factor is determined by:

$$c=\frac{\overline{v}}{\Gamma\left(1+\frac{1}{k}\right)} \quad (21)$$

Γ is gamma function. It expresses by:

$$\Gamma(x)=\int_0^{\infty}\exp(-t)t^{x-1}dt \quad (22)$$

The most probable (v_{mp}) and maximum energy carrying (v_{Emax}) wind speeds is given by [52]:

$$v_{mp}=c\left(\frac{k-1}{k}\right)^{1/k} \quad (23)$$

$$v_{Emax} = c\left(\frac{k+2}{k}\right)^{1/k} \quad (24)$$

2.2.2.2. Wind power density

This density represents the quantity of energy produced by the wind. The Weibull wind power density per unit area is expressed by [43, 52, 53]:

$$P = \frac{1}{2}\rho c^3 \Gamma\left(1+\frac{3}{k}\right) \quad (25)$$

P is the wind power ($W.m^{-2}$) and ρ is the air density at the site.

3. RESULTS AND DISCUSSION

3.1 Monthly daily profile of wind speed and temperature at the Conakry site

3.1.1 Vertical profile of minimum, maximum and average velocity

In Figure 2, the monthly vertical profile of minimum, maximum and average wind speeds for all stability classes are presented.

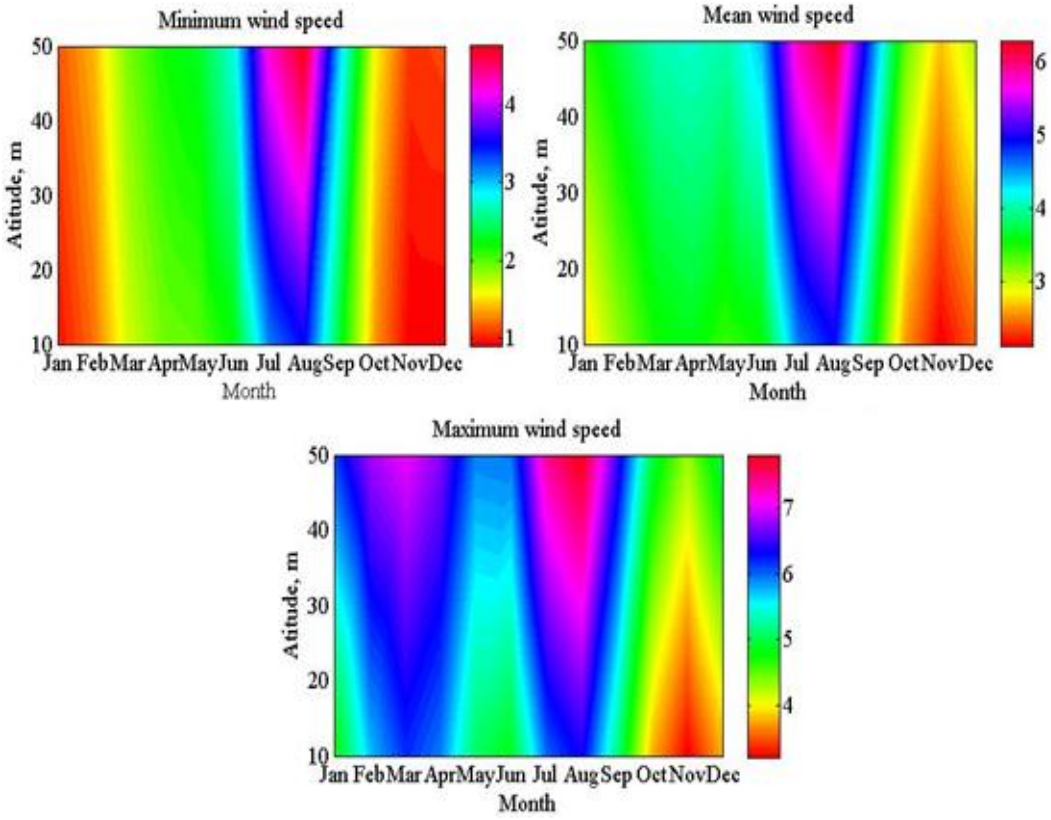

Fig. 2. Average vertical profile of minimum, average and maximum wind speed in Conakry (2001-2019)

The monthly vertical profile of wind speeds from 10 m to 50 m above the ground at the Conakry site indicates low values generally during the period from October to December. High values are observed especially during the months of July and August. The vertical profile of minimum velocities varies from 1 $m.s^{-1}$ (10 m) to 5 $m.s^{-1}$ (50 m) above the ground. During the period from October to December the wind speeds generally do not exceed 1.5 $m.s^{-1}$. From March to June and in September, they are between 1.5 $m.s^{-1}$ and 2.8 $m.s^{-1}$. Between the months of July and August the values go from 3 $m.s^{-1}$ to 5 $m.s^{-1}$. For the vertical profile of average wind speeds, the lowest values are obtained between November and December and are of the order of 2 to 3 $m.s^{-1}$ from 10 m to 50 m above the ground. During the months of January to June and September to October the average speeds vary from 3 $m.s^{-1}$ to 4.2 $m.s^{-1}$. In July, the speeds evolve from 4.2 $m.s^{-1}$ at 10 m to 5.5 $m.s^{-1}$ at 50 m above the ground and from 4.2 $m.s^{-1}$ to 6.1 $m.s^{-1}$ in August. On the vertical profile of maximum winds, the period from November to December always records the lowest speeds, which are between 3 $m.s^{-1}$ and 5 $m.s^{-1}$ from 10 m to 50 m above ground. From January to June and from September to October the profile varies from 4 $m.s^{-1}$ to 7 $m.s^{-1}$. In July-August, the maximum speeds are of the order of 6 $m.s^{-1}$ to 7.5 $m.s^{-1}$. The high wind speeds observed during the period of July-August and the lowest from October to December could be explained by the movement and position of the intertropical front (ITF) during the year in the West African region. Its northward movement in the lower atmosphere marks the arrival of the West African monsoon in late June, from a position of 15°N to another position at 19.3°N in July-August [54]. The presence of the West African monsoon at the coastal site of Conakry increases the local wind speeds, thus explaining the high values obtained during this period. During the November-December period, the ITD moves southward, dominating the West African monsoon. However, its intensity is low in the coastal regions of West Africa [3]. This observation would explain the low wind speeds observed during this period.

3.1.2 Temperature distribution of the ambient air

In Figure 3, the air temperature distribution is shown.

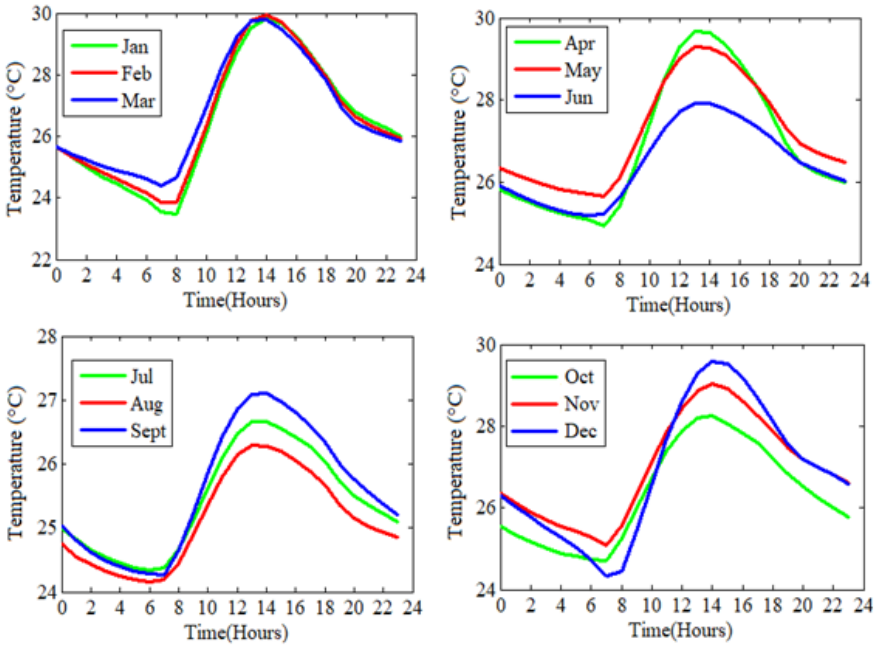

Fig. 3. Average air temperature profile at 10 m above ground in Conakry (2001-2019)

The figure 3 shows the daily variation of the ambient air temperature on a monthly scale. It can be seen that during the period from January to March the highest temperature values are recorded, especially during the day with peaks obtained around 01-02 p.m. in the order of 30°C. The lowest values collected in this period are observed around 08 a.m. with values between 23.4°C (January) and 25°C (March). This period, which corresponds to the dry season, explains these high values. From April to June, the peak of the period is obtained in April (29.5°C) around 01 p.m. In May this peak is 29°C and in June a little less than 28°C announcing the beginning of the rainy season. The lowest temperatures are recorded around 07 a.m. with values ranging from 25°C (April) to 25.8°C (May). From July to September the values are the lowest of the year because of the rainy season which is intense during this period. They vary from 24°C (August) at 7 a.m. to 27.1°C (September) around 01 p.m. From October to December, temperatures range from 24.2°C to 29.5°C obtained during the month of December (dry season period). The lowest peak observed at 01 p.m. over the period is recorded in October with a value of 28.1°C which announces the end of the rainy season.

3.2 Model for estimating the wind profile by atmospheric stability class

3.2.1 Variation of wind shear parameters

3.2.1.1 Wind shear coefficient

The variation of the ground wind shear coefficient observed between 10 m and 50 m on the Conakry is presented in Figure 4.

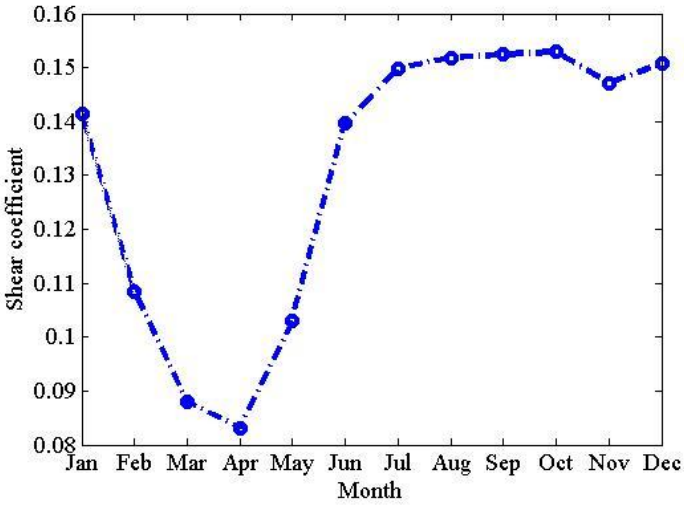

Fig. 4. Wind shear coefficient in Conakry (2001-2019)

The wind shear coefficient at the Conakry site shows seasonal variation. The lowest values of this coefficient are obtained during the months of March and April (0.085; 0.081). The highest values are observed between July and October around the value of 0.15. During the rainy season, the wind shear coefficient increases from 0.081 (April) to 0.151 (October) and during the dry season from November to April, it decreases from 0.148 to 0.081.

3.2.1.2 Friction speed and roughness length

From the logarithmic least squares regression, the X and Y fit coefficients are presented in Table 3.

Table 3 Least squares fitting parameters

	Jan	Feb	Mar	Apr	May	Jun	Jul	Aug	Sep	Oct	Nov	Dec
X	0.43	0.37	0.33	0.32	0.38	0.55	0.77	0.84	0.64	0.44	0.35	0.41
Y	1.73	2.28	2.73	2.85	2.51	2.24	2.79	2.97	2.24	1.54	1.30	1.46

Figure 5 shows the variation in ground roughness and friction velocity.

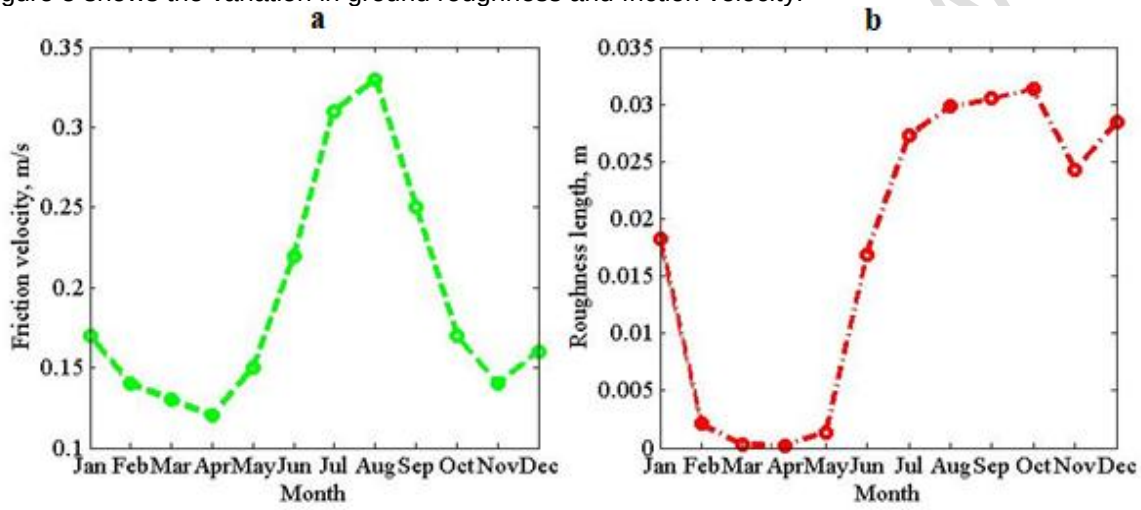

Fig. 5. Monthly variation of ground roughness and friction velocity in Conakry (2001-2019)

The variation of the wind friction velocity shows in Figure 5(a) a peak during the year recorded during the month of August. The lowest values are observed in the dry season with an average of 0.15 $m.s^{-1}$. During the rainy season, the velocity of friction is higher and the average is estimated at 0.23 $m.s^{-1}$. The average annual velocity of friction is estimated at 0.19 $m.s^{-1}$. On the coastal sites, Donnou et al [3], Peña and Gryning [55] and Jarmalavicius et al [56] obtained respectively the values of 0.38 $m.s^{-1}$; 0.55 $m.s^{-1}$, 0.43 $m.s^{-1}$ which are higher than those obtained in this study. This could be explained by the fact that in the work of Donnou et al [3], the authors studied the vertical wind profile only during the unstable period of the atmosphere. As for Peña and Gryning [55] on the west coast of Jutland in Denmark and Jarmalavicius et al [56] on the Baltic coast of Lithuania, the differences observed could be due to the temperate climate characterized by these European coasts. In Figure 5(b), we notice that the variation of the ground roughness and the wind shear coefficient are strongly correlated with a Pearson correlation coefficient evaluated at 0.96. The roughness varies from 10^{-4} m (April) to 0.0302 m (September). The average annual roughness length is 1.7 x 10^{-2} m. These low values could be due to changes in ground surface characteristics at the site relative to its cover [3]. Wind direction could also have a significant impact on the variability of ground roughness. In particular, the presence of buildings or obstacles at the wind measurement site would explain the high values recorded in July-September. Chang et al [57] and Donnou et al [3] obtained respectively 5 x 10^{-3} m and 7 x 10^{-3} m as a value of ground roughness at coastal sites. These results are close to those estimated in this study.

3.2.1.3 Atmosphere stability parameter

In the figure 6, the Obukhov length is determined and its evolution during a typical day on a monthly scale is presented.

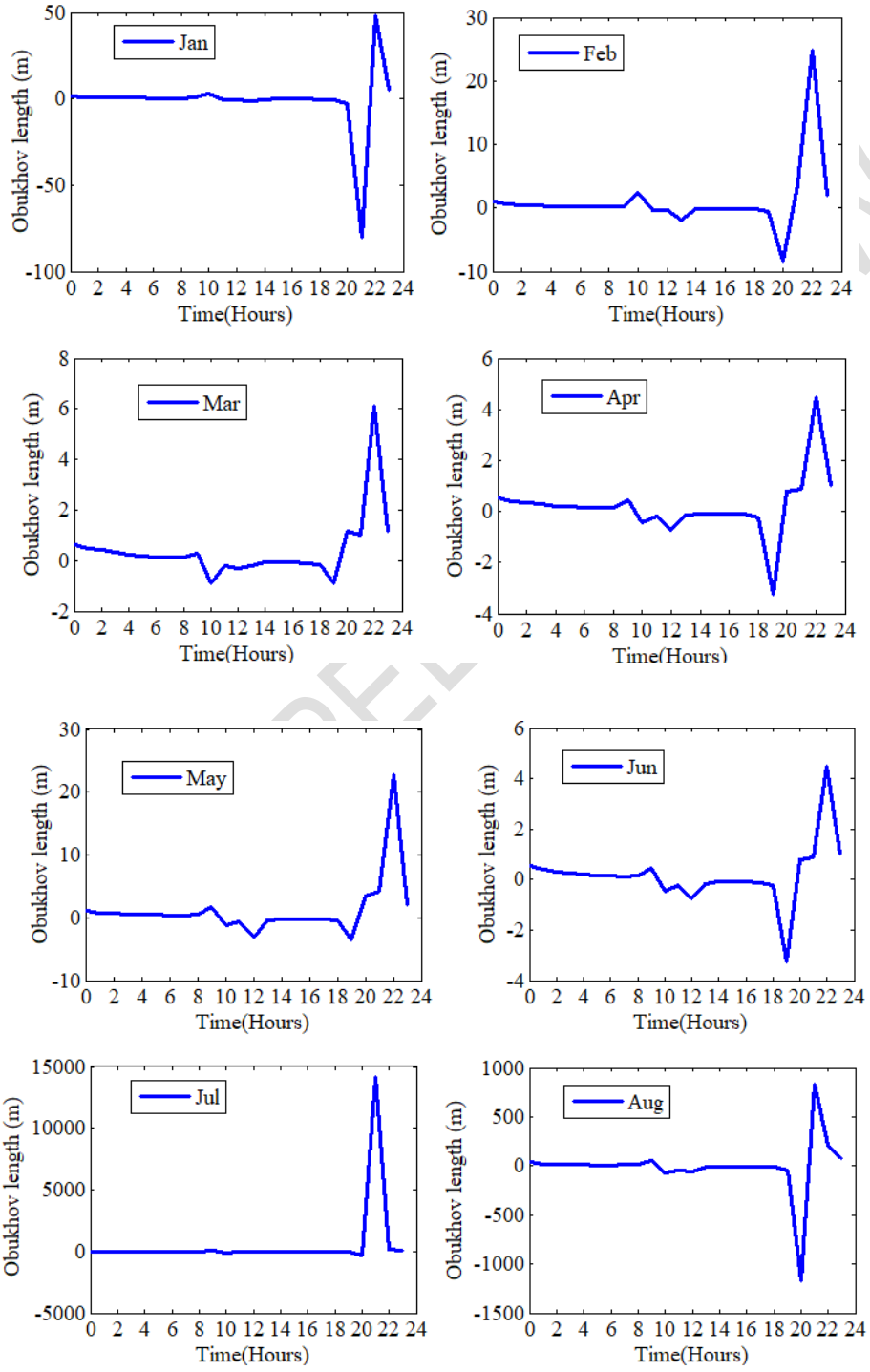

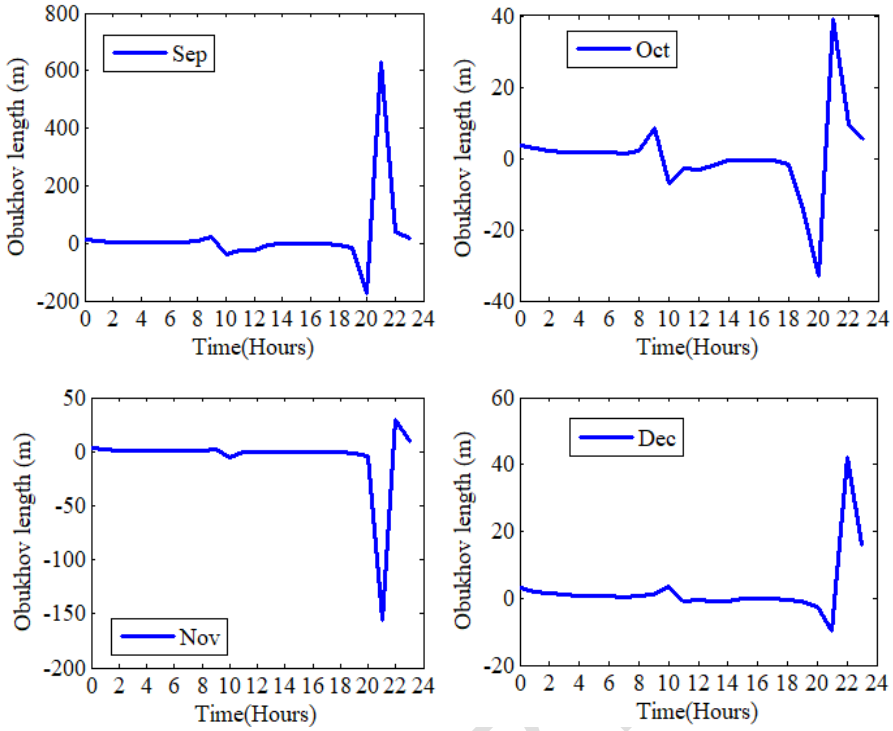

Fig. 6. Monthly variation of Obukhov length in Conakry (2001-2019)

During the year the values taken by the Obukhov length have allowed to characterize the stability of the atmosphere in stable and unstable periods. In general, the atmosphere remains stable at Conakry from 09 p.m. to 10 a.m. and unstable from 10 a.m. to 09 p.m. Indeed, during the day the air temperature decreases faster than the adiabatic gradient of air masses. The solar radiation reflected on the ground induces intense movements of the air masses with a high convection which leads to a disordered movement of the latter, responsible for the observed instability. At nightfall, with the disappearance of sunshine, these convective movements decrease and give way to orderly movements. They occur because the air temperature decreases less rapidly than the adiabatic gradient of the air masses. In this case, the air masses tend to descend towards the ground because of their rapid cooling. However, the cases of instability of the atmosphere observed during the night (until 09 p.m.) would be due to the cooling of the ground in the evening. Indeed during the day a part of the solar radiation is absorbed by the ground. At night, this heat is released by the ground and can lead to convective movements of air masses that warm up under the influence of this energy released into the atmosphere. It should be noted that these convective movements, less intense than during the day, could therefore explain the instability observed at this time. This characterisation of the atmosphere in Conakry is confirmed by the studies of Donnou et al [3], Boro et al [58], Gualtieri et al [4], Yahaya et al [59] and Fritz et al [60] who also estimate that the atmosphere is generally unstable during the day and stable during the night.

3.2.2 Model proposed on the site of Conakry

3.2.2.1 Estimation of wind profile by stability class

The variation of wind speed with altitude for the stable and unstable period of the atmosphere has been estimated in Figure 7 from 10 m to 80 m above the ground. It can be

seen that the wind speed is lower in the stable period and higher in the unstable period during the year. During the period from January to April between 10 m and 80 m, the wind speed varies from 1.96 $m.s^{-1}$ to 4.75 $m.s^{-1}$ (stable period) and from 3.36 $m.s^{-1}$ to 7.1 $m.s^{-1}$ (unstable period). From May to August and during the unstable period, the profile varies from 4.13 $m.s^{-1}$ (May) to 8.79 $m.s^{-1}$ (August) from 10 m to 80 m. During the stable period (between 10 m and 80 m), it varies from 2.36 $m.s^{-1}$ (June) to 4.82 $m.s^{-1}$ (August). During the unstable and stable period from September to December, the wind speeds vary respectively from (2.35 $m.s^{-1}$; 1.66 $m.s^{-1}$) in November to (6.74 $m.s^{-1}$; 3.91 $m.s^{-1}$) obtained in September from 10 to 80 m. The annual average wind speed at 10 m during the stable and unstable period of the atmosphere is estimated at (2.28 $m.s^{-1}$; 3.51 $m.s^{-1}$) respectively. At 80 m, it is estimated respectively at (3.94 $m.s^{-1}$; 6.3 $m.s^{-1}$). The high wind speeds observed during the day at the coastal site of Conakry are due to local breezes, particularly the sea breeze, which is a thermal wind that occurs during the day and is generally intense. During the night until the morning before the appearance of the sun the land breeze present and less intense would explain the low wind speeds of the stable period. In several coastal regions of West Africa, some authors have evaluated the average wind speed at different altitudes. Salami et al [61] obtained respectively annual mean values of 3.5 $m.s^{-1}$ and 4.16 $m.s^{-1}$ at 10 m in Lome and Accra during a typical day. In the studies of Donnou et al [52] for the unstable period of the atmosphere at the coastal site of Cotonou, the average wind speed is between 2.8 $m.s^{-1}$ and 8.5 $m.s^{-1}$ from 10 m to 60 m above ground. At the sites of Kayar, Potou, Gandon, Sine Moussa Abdou, Botla, Dara Andal, Nguebeul and Sakhor in northwestern Senegal, Ouldbilal et al [62] and Ouldbilal et al [63] indicated in their studies that the diurnal wind speed was higher than the nocturnal wind speed, thus confirming the variations observed in Conakry. Between 12 m and 20 m the wind speed varied from 4.83 $m.s^{-1}$ obtained at Botla to 5.69 $m.s^{-1}$ observed at Nguebeul. At several sites in Ghana (Adafoah, Anloga, Aplaku, Mankoadze, Oshiyie and Warabeba), the annual mean wind speeds independently of atmospheric stability conditions were estimated respectively at 5.30 $m.s^{-1}$, 4.50 $m.s^{-1}$, 4.75 $m.s^{-1}$, 4.51 $m.s^{-1}$, 3.88 $m.s^{-1}$ and 4 $m.s^{-1}$ at 12 m from the ground by Adaramola et al [64]. In Nigeria, many authors such as Na et al [65] on the coastal sites of Calabar, Uyo, Warri and Ikeja, Oluleye and Ogungbenro [15] on the coastal sites of Lagos and Calabar have obtained velocities ranging from 3.88 $m.s^{-1}$ (10 m) to 9 $m.s^{-1}$ (70 m). During the diurnal and nocturnal cycle, Youm et al [66] estimated at 10 m the wind speeds of (4.48; 3.09) $m.s^{-1}$ in Mboro and (5.28; 4.36) $m.s^{-1}$ in Makhana. These different values are in agreement with those obtained at Conakry, although it should be noted that at some coastal sites, wind speeds were higher than at Conakry.

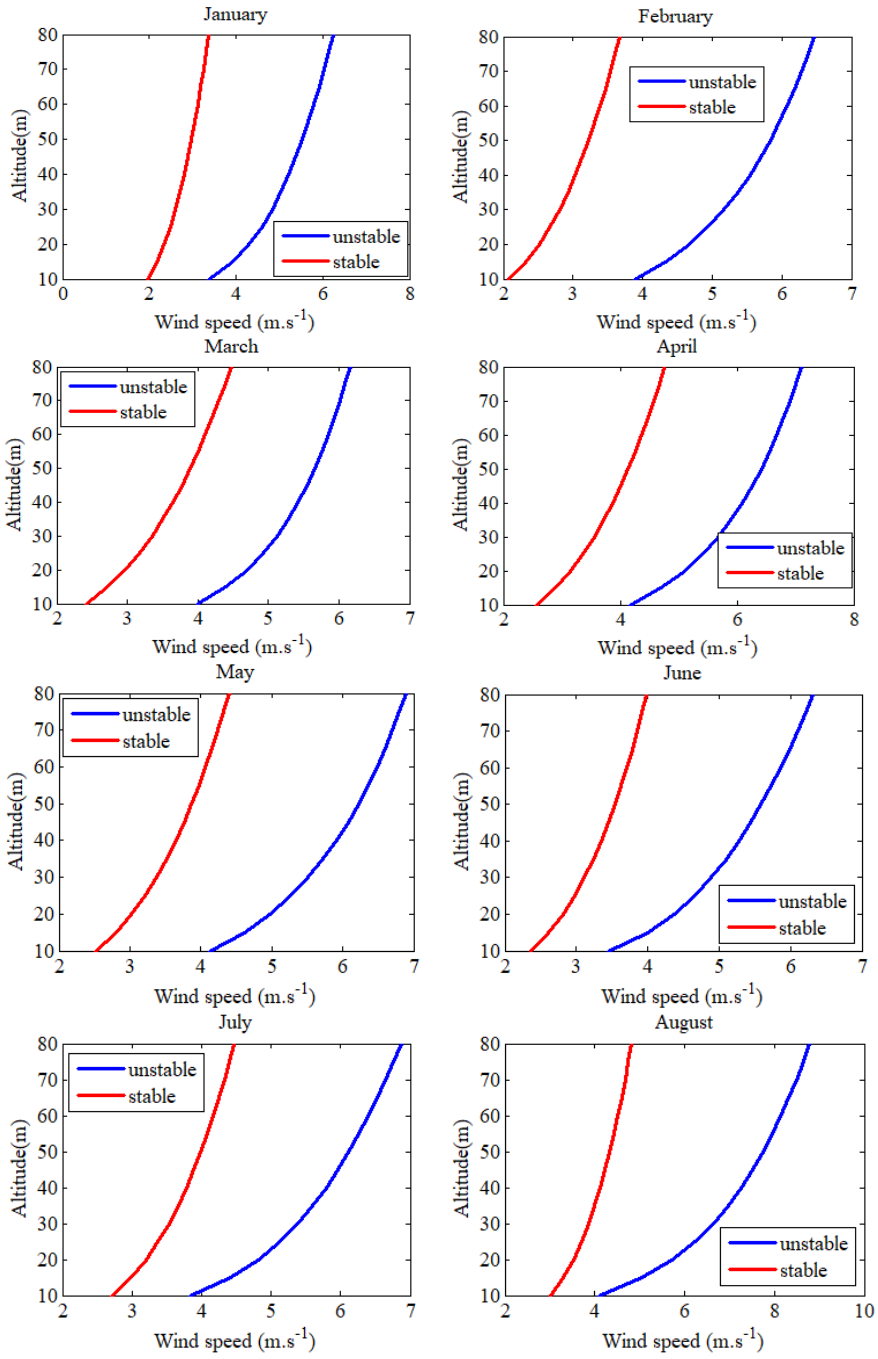
January
February
March
April
May
June
July
August
Altitude(m)
Wind speed (m.s-1)
unstable
stable

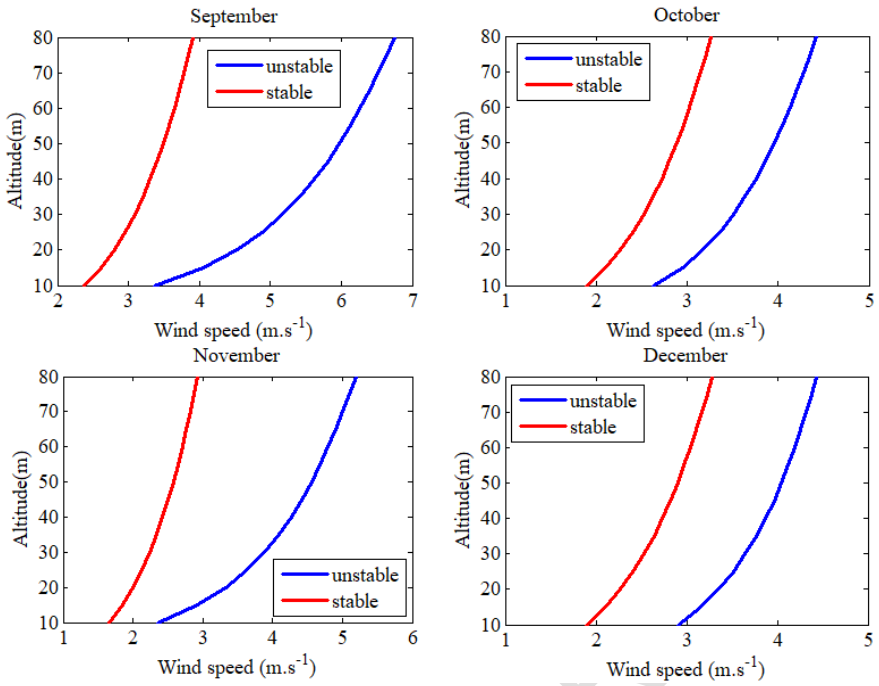

Fig. 7. Vertical wind profile for the stable and unstable period of the atmosphere in Conakry (2001-2019)

3.2.2.2 Characterisation of the vertical wind profile

Using the Nelder and Mead simplex algorithm, the vertical wind profile model was fitted with the measurements from the proposed wind shear coefficient formulation in equation (15). The profile characterisation is presented in Figures 8 and 9 with the different calibration coefficients. The analysis of the error estimators (RMSE and MAE) indicate overall low values regardless of the stable period of the atmosphere. During the unstable period from January to June the root mean square error varies from 0.05 $m.s^{-1}$ to 0.08 $m.s^{-1}$ and the mean absolute error from 0.03 $m.s^{-1}$ to 0.07 $m.s^{-1}$. During July, October and December, the RMSE ranges from 0.01 $m.s^{-1}$ to 0.09 $m.s^{-1}$ and from 0.009 $m.s^{-1}$ to 0.06 $m.s^{-1}$ for the MAE. In August, September and November the error estimators are higher and vary respectively from 0.16 to 0.25 $m.s^{-1}$ (RMSE) and from 0.14 to 0.22 $m.s^{-1}$ (MAE). August is the month with the highest value of error estimators and in December we observe the best fit of the wind shear model during the year. For the stable period of the year, the error estimators are lower than the unstable period and are of the order from 10^{-3} to 10^{-5} $m.s^{-1}$. The average wind shear coefficient in the stable period is 0.26 and in the unstable period is estimated at 0.28. Referring to the studies of Donnou et al [3] on the coast of Cotonou under a convective atmosphere, the authors obtained a wind shear coefficient estimated at 0.20. Gualtieri and Secci [16] after comparing several methods of estimating the stability of the atmosphere in a coastal and industrial area located in southern Italy obtained as wind shear coefficient respectively 0.176 and 0.326 for the unstable and stable period. Rehman and Al-Abbadi [7] estimated the wind shear coefficient in Saudi Arabia from measurements at 20, 30 and 40 m from the ground. The average shear coefficient was found to be 0.194 with high values in stable period. These different values are close to those obtained in Conakry and therefore confirm the results of wind shear. Table 3 presents the monthly values of the calibration coefficients of the wind shear model for each class of the atmosphere stability. Based on these site-specific adjustment coefficients, the proposed wind shear formulation combined

with the power law now constitutes a reliable model for estimating the wind speed at an altitude greater than 10 m above the ground in the surface boundary layer at Conakry.

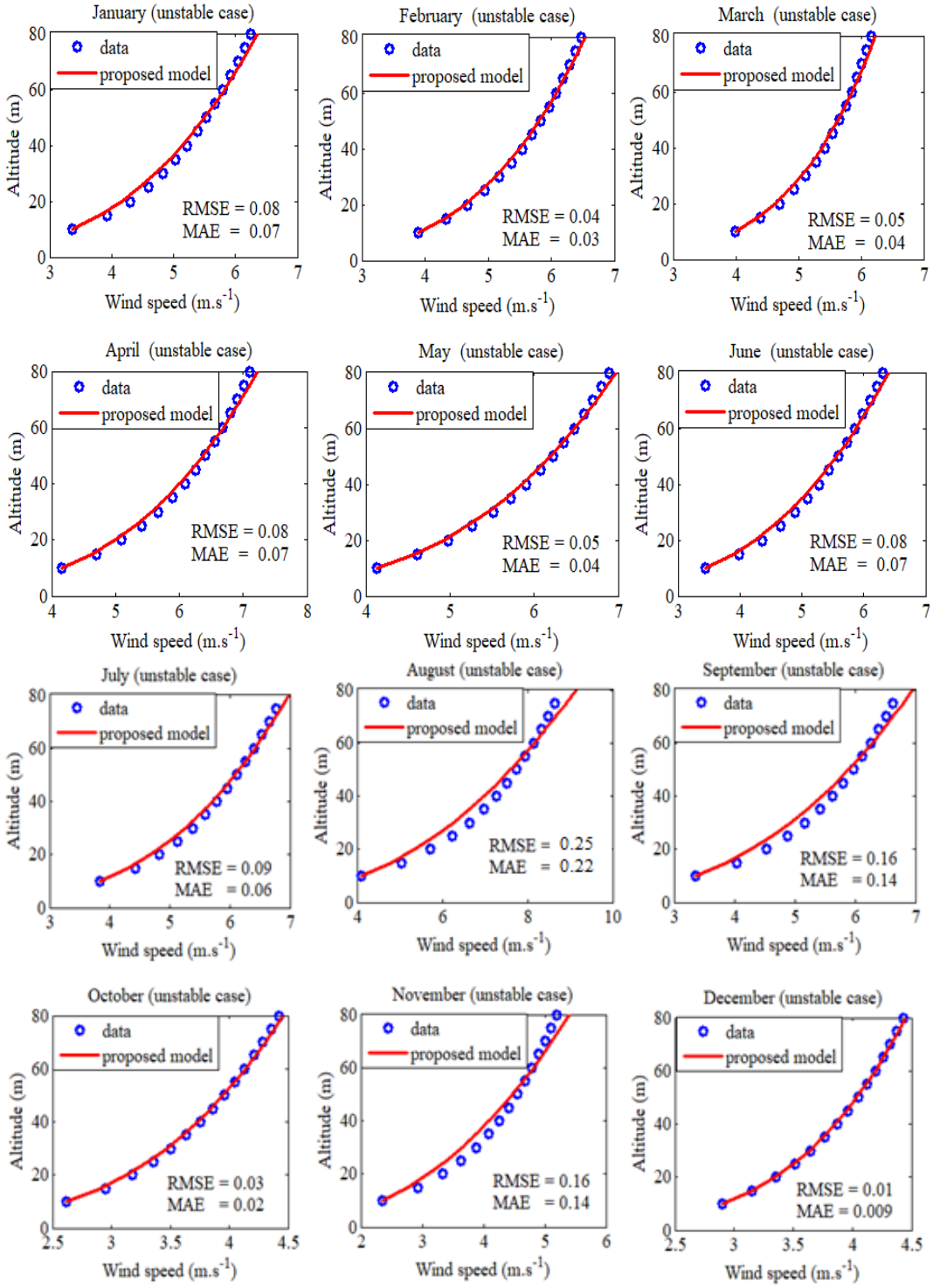

Fig. 8. Adjustment of the vertical wind profile for the unstable period of the atmosphere in Conakry (2001-2019)

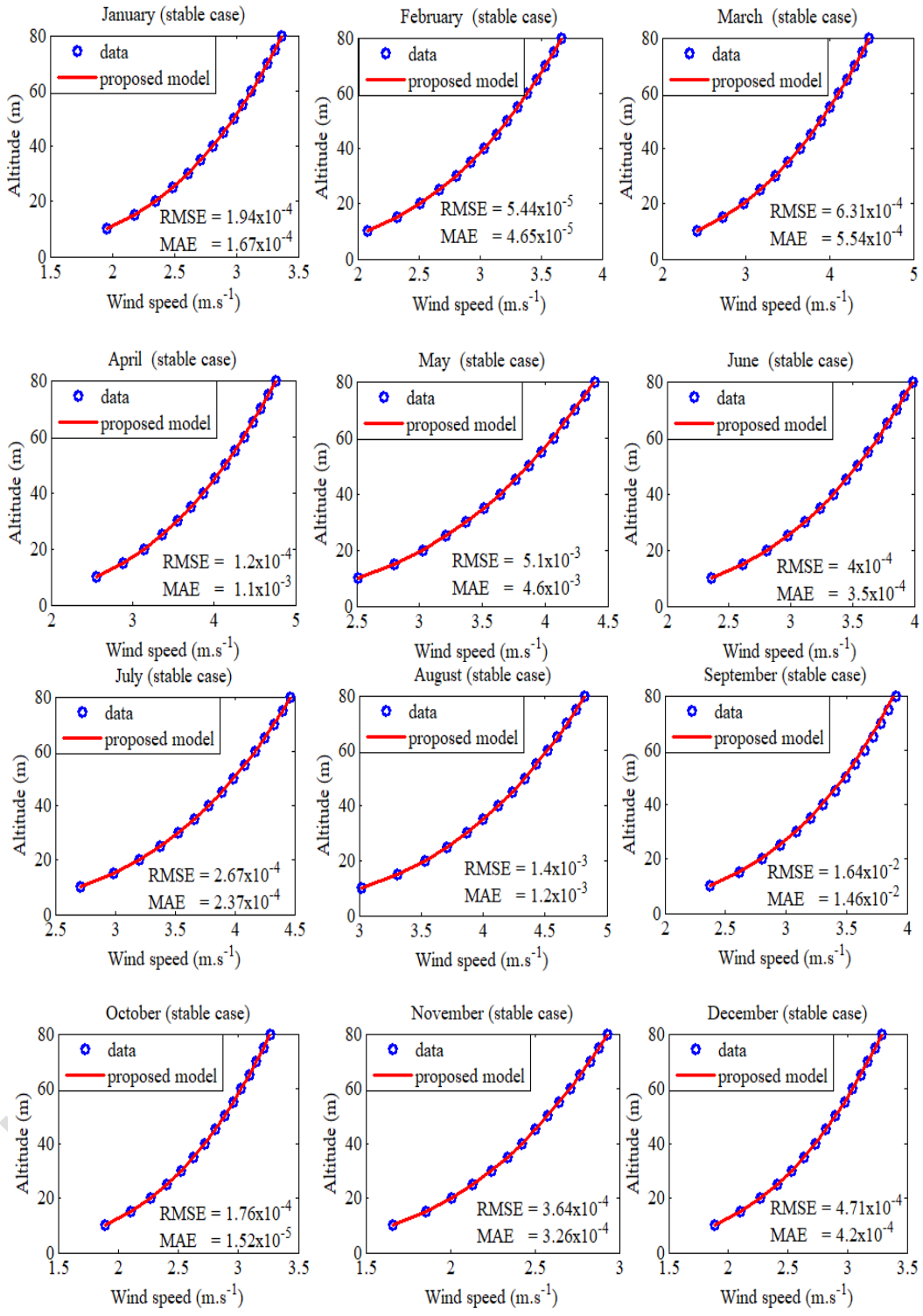

Fig. 9. Adjustment of the vertical wind profile for the stable period of the atmosphere in Conakry (2001-2019)

Table 4 Fitting coefficients of the proposed model

	Atmosphere stable				Atmosphere unstable			
Month	a	B	c	d	A	B	c	d
January	0.088	-0.013	-0.049	0.21	0.053	-0.715	0.184	0.0660
February	0.10	-0.106	-0.26	0.153	0.009	0.09	0.018	0.164
March	0.005	0.001	0.068	0.117	-0.02	0.116	0.010	0.147
April	0.067	0.0105	0.025	0.105	-1.57	-0.567	-0.325	0.131
May	0.078	0.004	0.047	0.148	0.019	0.018	0.09	0.155
June	0.077	-0.103	-0.105	0.193	0.08	-0.012	0.018	0.187
July	0.057	-0.010	-0.018	0.237	0.084	-0.005	0.068	0.208
August	0.127	-0.073	-0.263	0.213	0.11	-0.057	0.056	0.133
September	0.086	-0.424	-0.015	0.067	0.024	-0.018	0.091	0.177
October	0.083	-0.62	0.013	0.071	0.044	-0.076	0.088	0.225
November	0.108	-0.063	-0.037	0.204	0.053	-0.318	0.011	0.022
December	0.002	0.002	0.099	0.226	-0.03	-0.13	0.053	0.273

3.3. Comparative study of the models

The performance of the proposed model for Conakry has been compared to some existing models in the literature whose characteristic parameters have been determined for the Conakry site. The different wind profiles are presented in Figure10.

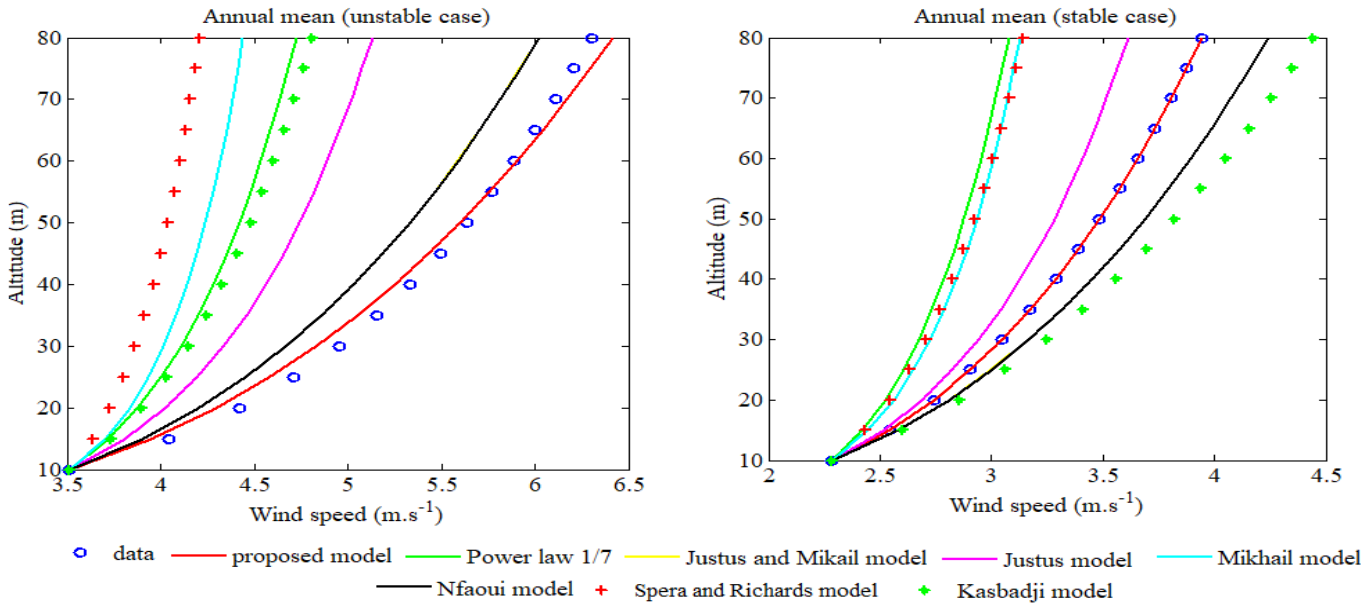

Fig. 10. Comparison of the vertical wind profile for the stable and unstable period of the atmosphere with different models in Conakry (2001-2019)

The error estimators from the different models mentioned above are presented in Table 5.

Table 5 Values of error estimators

	Atmosphere stable		Atmosphere unstable	
Month	MAE	RMSE	MAE	RMSE
Proposed model	$3.8x10^{-4}$	$4.5x10^{-4}$	0.07	0.09
Power law 1/7	0.51	0.58	1.03	1.12
Justus and Mikhail model [8]	0.17	0.19	0.26	0.27
Justus model [67]	0.14	0.20	0.76	0.83
Mikhail model [9]	0.47	0.59	1.18	1.3
Nfaoui model [10]	0.17	0.19	0.26	0.27
Spera and Richards model [38]	0.48	0.53	1.35	1.48
Kasbadji Model [11]	0.28	0.32	0.98	1.07

The wind shear formulation proposed in this study gives a better estimate of wind speed as a function of altitude with the lowest values of RMSE and MAE ($4.5x10^{-4}$; $3.8x10^{-4}$) $m.s^{-1}$ in stable and unstable periods (0.09; 0.07) $m.s^{-1}$. The models encountered in the literature all underestimated the vertical wind profile in unstable periods. In stable period except the models of Nfaoui and Kasbadji which overestimate the wind speeds in altitude, all other models also underestimate it. However, the models of Nfaoui and Justus and Mikhail whose error estimates vary from 0.17 $m.s^{-1}$ to 0.27 $m.s^{-1}$ are the only estimates from the literature that seem to be the closest to the measurements. The results of this comparative study confirm the establishment of an appropriate model for each site considered as recommended by several authors.

3.4. Variation of the Wind Potential

3.4.1 Variation of Weibull parameters by stability class

The Weibull parameters k and c determined by atmospheric stability class are presented in Figures 11 and 12. Both parameters are increasing functions of altitude for all atmospheric stability classes. However, the k parameter increases very little with altitude, unlike the scale parameter, which has a higher vertical wind gradient. During the dry season from November to mid-May, k varies from 1.27 (November) to 2.21 (April) for the unstable period and from 1.06 (November) to 1.81 (April) for the stable period from 10 m to 80 m. During the rainy season from mid-May to October (stable and unstable period), we notice that k evolves respectively from (1.14; 1.34) obtained in October to (1.82; 2.46) observed in August. As for the scale parameter from 10 m to 80 m, it varies from 2.85 $m.s^{-1}$ (October) to 9.9 $m.s^{-1}$ (August) during the diurnal convective cycle and from 1.98 $m.s^{-1}$ (October) to 5.42 $m.s^{-1}$ (August) during the nocturnal cycle. These values are recorded during the rainy season. In the dry season (stable period), the minimum scale parameter is 1.70 $m.s^{-1}$ (November) at 10 m and 5.35 $m.s^{-1}$ at 80 m for its maximum value. In unstable period, it varies from 2.53 $m.s^{-1}$ (November) to 8.02 $m.s^{-1}$ (August). The mean annual shape parameter (stable period) is between 1.25 (10m) and 1.64 (80 m) and during the unstable period, it varies from 1.55 to 2.07. The mean annual scale parameter at 10 m and 80 m is (3.9; 7.10) $m.s^{-1}$ (unstable atmosphere) and (2.45; 4.41) $m.s^{-1}$ when the atmosphere is stable. The low values of k ($k \leq 2$) obtained indicate a narrow distribution of winds around the mean. When $k \geq 2$ and $c \geq 2$ $m.s^{-1}$, a scattering of the data is observed [51]. Periods of strong wind generally correspond to high values of the shape parameter. When the wind is therefore frequent at a site, the Weibull parameters associated with this site are high. This result is confirmed by Donnou et al [52] and Ajavon et al [68].

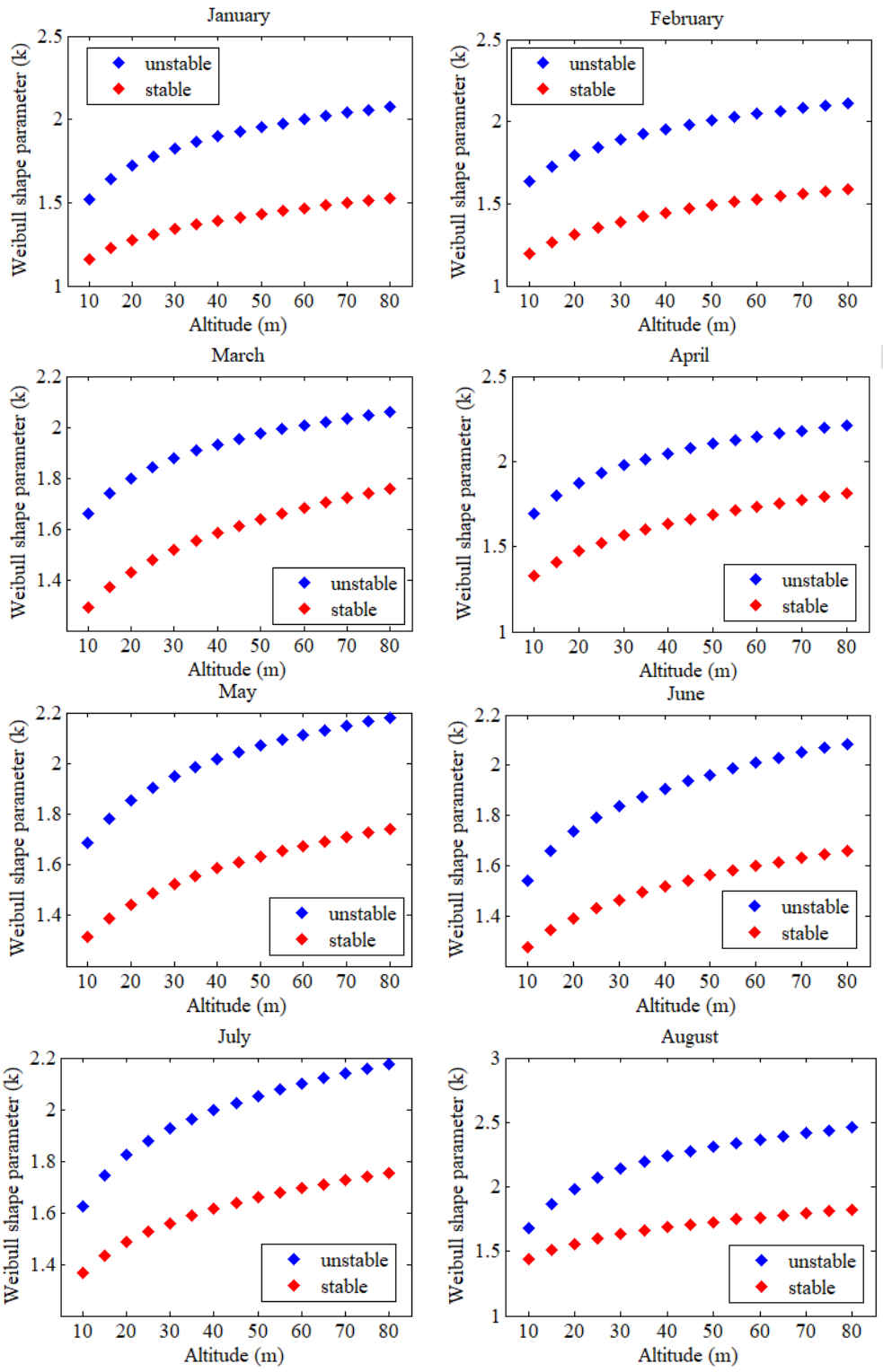
January
February
March
April
May
June
July
August
unstable
stable
Weibull shape parameter (k)
Altitude (m)

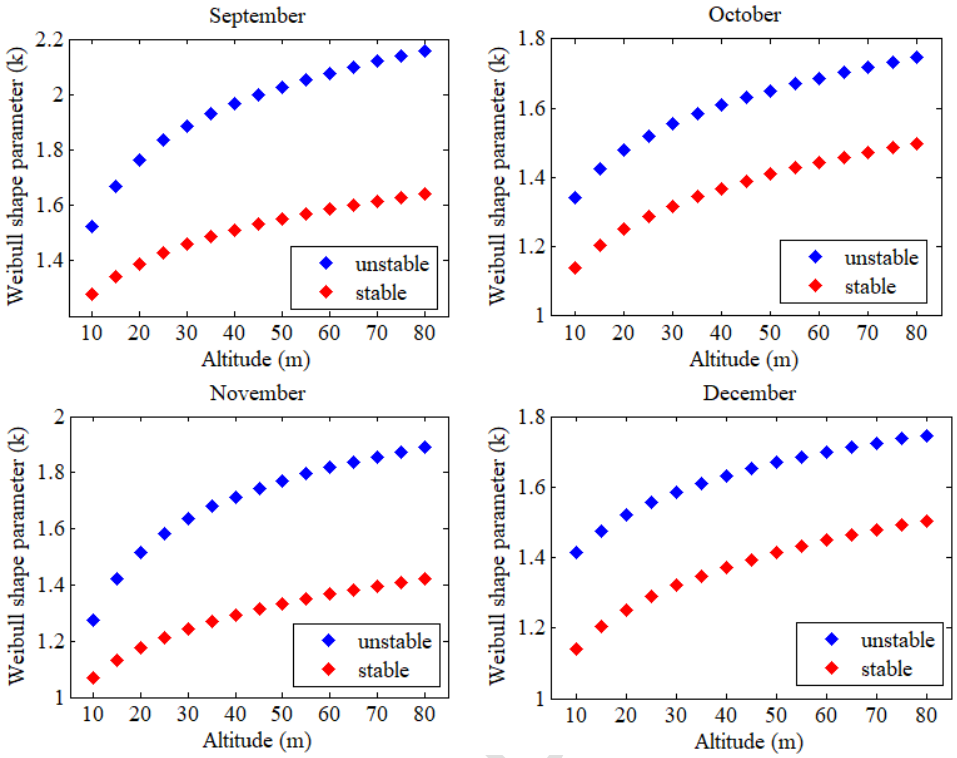

Fig. 11. Monthly variation of k during the stable and unstable period of the atmosphere in Conakry (2001-2019)

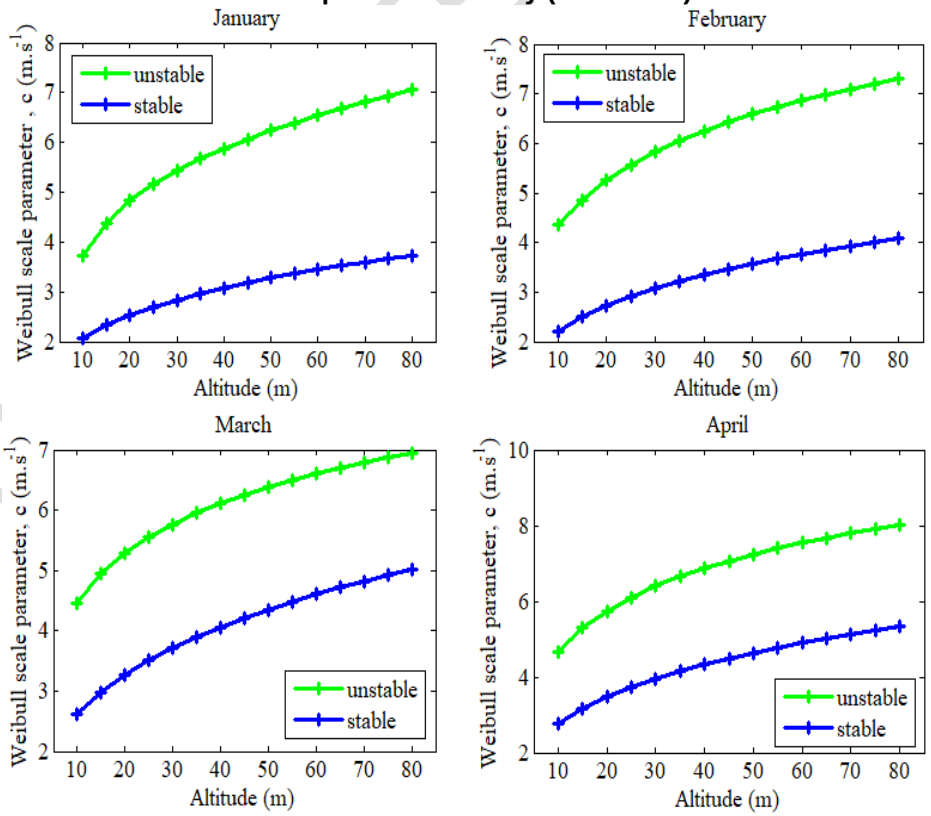

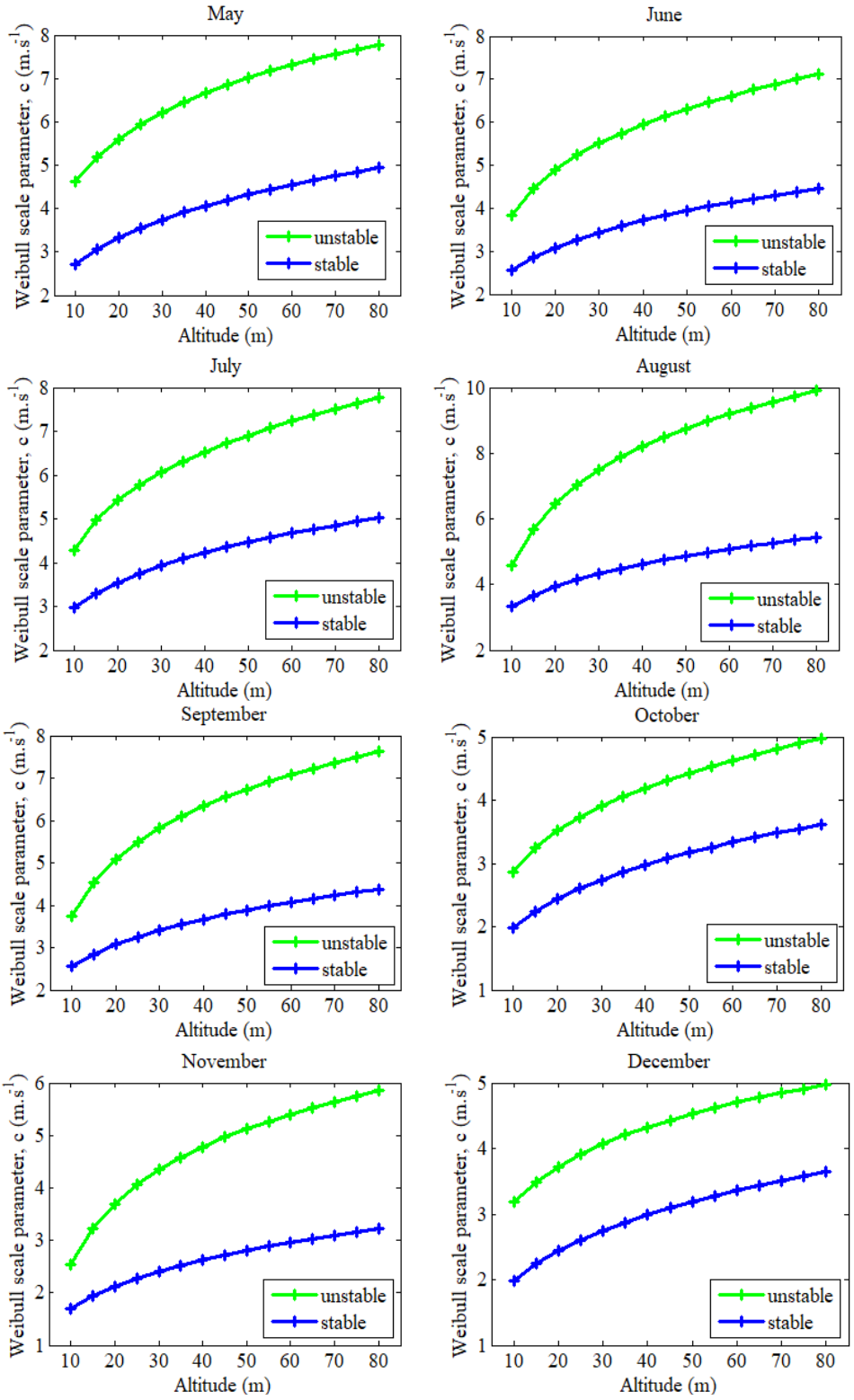

Fig. 12. Monthly variation of c during the stable and unstable period of the atmosphere in Conakry (2001-2019)

3.4.2 Wind Energy Distribution

The wind energy that can be expected in Conakry for each class of atmospheric stability was determined at a monthly scale. The variation of this energy is shown in Figure 13. During the period from November to mid-May (dry season), the production of wind energy is more important during the day than night. During the dry season (unstable period), the highest amounts of energy are observed during the month of April with values ranging from 102 $W.m^{-2}$ (10m) to 383 $W.m^{-2}$ (80m). The lowest amounts recorded in November-December are estimated at 28 $W.m^{-2}$ (November) and 118 $W.m^{-2}$ (December) at 10m and 80m respectively. The average power density during this season (unstable period) is 69 $W.m^{-2}$ at 10 m above ground and 252 $W.m^{-2}$ at 80 m. During the stable period of the atmosphere at 10 m from the ground, the power density varies from 14 $W.m^{-2}$ (November) to 34 $W.m^{-2}$ (April). At 80 m from the ground, it evolves from 46 $W.m^{-2}$ (November) to 140 $W.m^{-2}$ (April). The seasonal average density (stable period) is 23 $W.m^{-2}$ at 10 m and 84 $W.m^{-2}$ at 80 m. From mid-May to October (rainy season), the energy production is much higher in August with a power density of 664 $W.m^{-2}$ at 80 m during the day. During the night cycle, it is estimated at 145 $W.m^{-2}$ (80 m). In October less energy is produced compared to the other months of the rainy season. We observe a power density of 118 $W.m^{-2}$ at 80 m and 36 $W.m^{-2}$ at 10 m. The average seasonal density (stable period) is estimated at 33 $W.m^{-2}$ (10 m) and 104 $W.m^{-2}$ (80 m) and from 74 $W.m^{-2}$ (10 m) to 350 $W.m^{-2}$ (80 m) during the unstable period. Over the year, the energy production is maximum during the rainy season and more precisely in August. It is minimal in the dry season, especially in the months of November-December. The average annual energy production under a convective atmosphere at 10 m and 80 m is respectively 72 $W.m^{-2}$ and 301 $W.m^{-2}$. During the night cycle, this annual production varies from 28 $W.m^{-2}$ to 93 $W.m^{-2}$ from 10 m to 80 m.

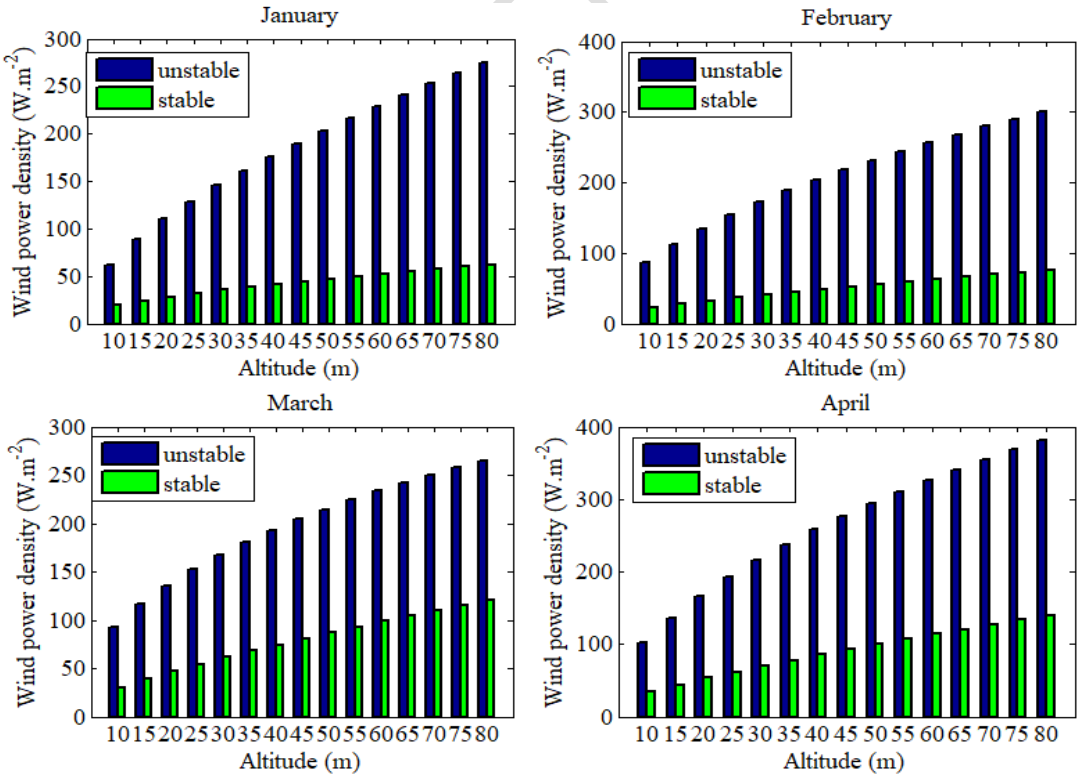

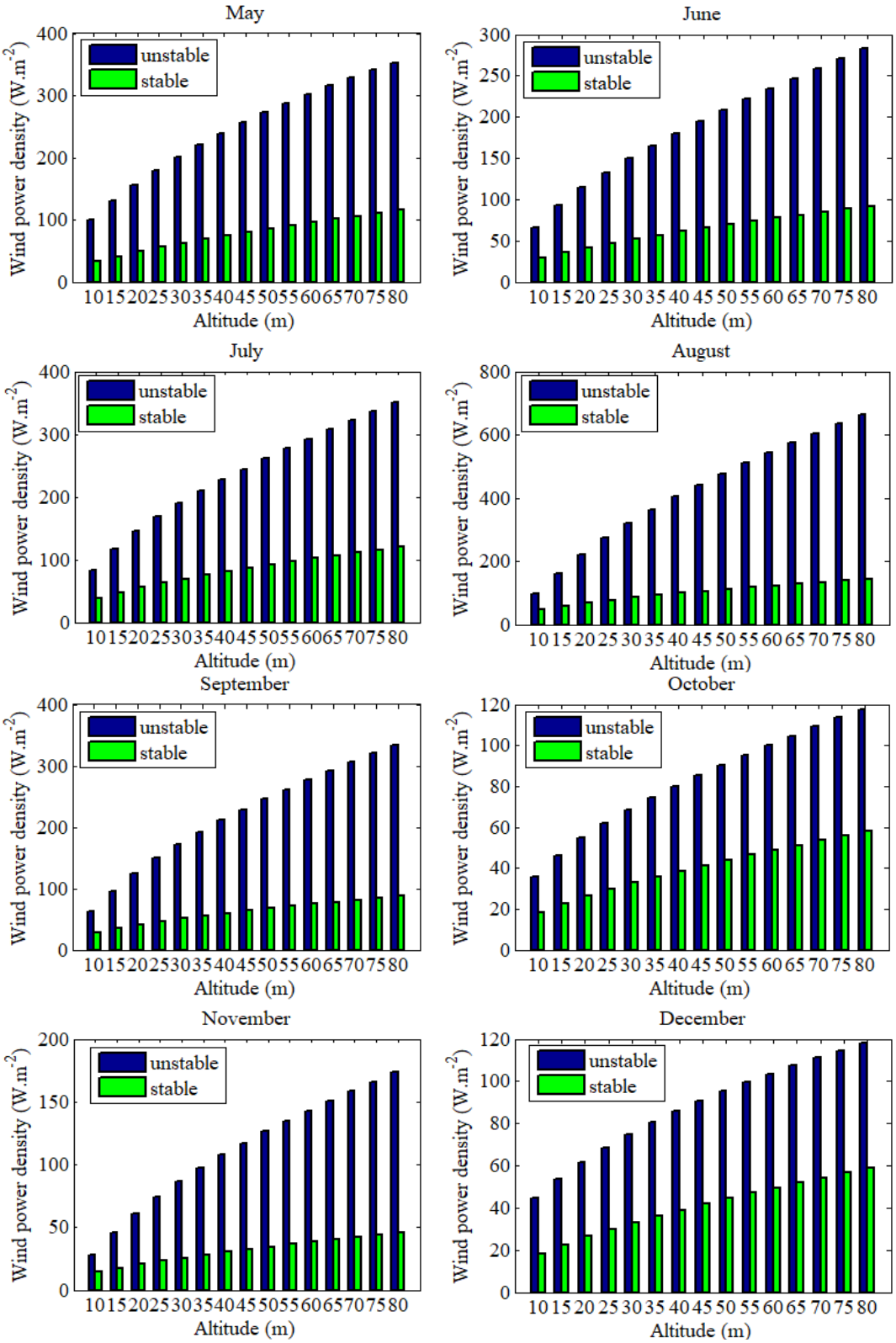

Fig. 13. Monthly variation of wind energy for the stable and unstable period of the atmosphere in Conakry (2001-2019)

Ouldbilal et al [62] and Ouldbilal et al [63] evaluated the annual daytime wind potential respectively at 99.64 $W.m^{-2}$, 145.30 $W.m^{-2}$, 103.14 $W.m^{-2}$ at 20 m, at 128.59 $W.m^{-2}$, 107.74 $W.m^{-2}$, 106.61 $W.m^{-2}$ and 117.53 $W.m^{-2}$ at 10 m and 143 $W.m^{-2}$ (12m) at the coastal sites of Kayar, Potou, Gandon, Botla, Dara Andal, Nguebeul, Sakhor and Sine Moussa in Senegal. At the coastal site of Cotonou in Benin, Donnou et al [52] evaluated the annual power density from 10 m to 60 m under a convective atmosphere. The values obtained indicate an average of 131 $W.m^{-2}$ at 10 m and 332.67 $W.m^{-2}$ at 60 m above ground. On the coastal site of Lome at 10 m, 30 m and 50 m, the annual potential is evaluated respectively at 64.52 $W.m^{-2}$, 103.08 $W.m^{-2}$, 130.41 $W.m^{-2}$ by Salami et al [61]. At the coastal sites of Accra (Anloga, Aplaku, Mankoadze, Oshiyie, Warabeba) in Ghana at 10 m, Adaramola et al [64] estimated the wind power density respectively at 97.75 $W.m^{-2}$, 107.19 $W.m^{-2}$, 105.19 $W.m^{-2}$, 98.04 $W.m^{-2}$, 61.10 $W.m^{-2}$ and 78.46 $W.m^{-2}$ at 10 m from the ground. In Calabar, Uyo and Warri in Nigeria, the wind potential is estimated at 21.4 $W.m^{-2}$, 48.9 $W.m^{-2}$ and 23.6 $W.m^{-2}$ at 10 m respectively by Na et al [65]. Comparing these values to those obtained in Conakry, we notice that the wind energy densities are similar. However, higher values can be reported at some coastal sites, notably in Senegal. These results are in good agreement with the wind energy potential in Conakry.

In sum, based on the wind power density classes used in the studies of Donnou et al [52] and Boro et al [58], the power densities calculated at the Conakry site belong to class 3 (300 $W.m^{-2}$; 400 $W.m^{-2}$) which is suitable for most wind power applications. The Conakry site is therefore suitable for medium power wind turbine installations for electricity and water production.

4. CONCLUSION

In this study, the vertical wind profile was characterized at the Conakry site for each stability class of the atmosphere and the wind potential was determined. The wind shear parameters were determined. Starting from the wind shear model of Newman and Klein, a new formulation of this parameter was proposed as a function of the Obukhov length at order 2 and calibrated with the simplex algorithm of Nelder and Mead. From the Weibull parameters obtained for the stable and unstable period of the atmosphere, the available wind potential in Conakry was estimated from 10 m to 80 m. The main results of this study are summarized as follows:

(1) The annual average wind speed at 10 m above the ground during the stable and unstable period of the atmosphere is estimated respectively at (2.28; 3.51) $m.s^{-1}$. At 80 m, it is estimated respectively at (3.94; 6.3) $m.s^{-1}$.

(2) The annual average of the ground roughness length is 1.7 x 10^{-2} m. The annual average of the ground friction speed is estimated at 0.19 $m.s^{-1}$. The atmosphere remains stable at the Conakry site from 09 p.m. to 10 a.m. and unstable from 10 a. m. to 09 p. m.

(3) The wind shear formulation proposed in this study gives a better estimate of wind speed as a function of altitude with the lowest values of RMSE and MAE ($4.5x10^{-4}$; $3.8x10^{-4}$) $m.s^{-1}$ in stable and unstable periods (0.09; 0.07) $m.s^{-1}$ compared to some models encountered in the literature. The annual mean of the wind shear coefficient in stable period is 0.26 and in unstable period evaluated at 0.28.

(4) The annual mean of the shape parameter from 10 m to 80 m in the stable period of the atmosphere is between 1.25 and 1.64 and during the unstable period it varies from 1.55 to 2.07. The annual mean of the scale parameter at 10 and 80 m is (3.9; 7.10) $m.s^{-1}$ (unstable atmosphere) and (2.45; 4.41) $m.s^{-1}$ when the atmosphere is stable.

(5) The annual average of the energy production under a convective atmosphere at 10 m and 80 m is estimated at 72 $W.m^{-2}$ and 301 $W.m^{-2}$ respectively. During the night cycle, this annual production varies from 28 $W.m^{-2}$ (10m) to 93 $W.m^{-2}$ (80 m).

These results now constitute a reliable database for wind turbine designers and installers in order to allow them to better characterize the different types of wind turbines among the average sizes that are suitable for the Conakry site.

However, the availability of the wind speeds at the scale of one hour at 50 m above the ground would have improved the performance of the model proposed in this study.

REFERENCES

1. Ismaiel, AMM and Yoshida S. Study of turbulence intensity effect on the fatigue lifetime of wind turbines. Journal of Novel Carbon Resource Sciences & Green Asia Strategy. 2018; 05(1):25-32.
2. Xu C, Hao C, Li L, Han X, Xue F, Sun M and Shen W. Evaluation of the Power-Law Wind-Speed Extrapolation Method with Atmospheric Stability Classification Methods for Flows over Different Terrain Types. Applied sciences. 2018; 1429(8):1-16.
3. Donnou HEV, Akpo AB, Kouchadé CA, Kounouhewa BB, Hounguè GH, Nonfodji GF, and Djossou J. Vertical Profile of Wind Diurnal Cycle in the Surface Boundary Layer over the Coast of Cotonou, Benin, under a Convective Atmosphere. Advances in Meteorology. 2019; 2019:1-18.
4. Gualtieri G and Secci S. Extrapolating wind speed time series vs. Weibull distribution to assess wind resource to the turbine hub height: a case study on coastal location in Southern Italy. Renewable Energy. 2014; 62:164-176.
5. Motta M, Barthelmie RJ, Vølund P. The influence of non-logarithmic wind speed profiles on potential power output at Danish offshore sites. Wind Energy. 2005; 8: 219-236.
6. En Z, Altunkaynak A, Erdik T. Wind Velocity Vertical Extrapolation by Extended Power Law. Adv. Meteorol. 2012; 2012:885-901.
7. Rehman S, Al-Abbadi NM. Wind shear coefficients and their effect on energy production. Energy Convers. Manag. 2005; 46:2578-2591.
8. Justus CG and Mikhail A. Height variation of wind speed and wind distributions statistics. Geophysical Research Letters. 1976; 3(5):261-264.
9. Mikhail AS. Height extrapolation of wind data. Journal of Solar Energy Engineering. 1985. 107(1):10-14.
10. Nfaoui H, Bahraoui BJ and Sayigh AAM. Wind characteristics and wind energy potential in Morocco. Solar Energy. 1998; 63(1):51-60.
11. Kasbadji NM. Evaluation du gisement énergétique éolien–contribution à la détermination du profil vertical de la vitesse du vent. These de Doctorat, Université Abou BekrBelkaıd de Tlemcen, Tlemcen, Algerie, 2006.
12. Rehman S and Al-Abbadi NM. Wind shear coefficient, turbulence intensity and wind power potential assessment for Dhulom, Saudi Arabia. Renewable Energy. 2008; 33(12):2653-2660.
13. Omer AM. On the wind energy resources of Sudan. Renewable and Sustainable Energy Reviews. 2008;12(8): 2117-2139.

14. Lackner MA, Rogers AL, Manwell JF, and McGowan JG. A new method for improved hub heightmean wind speed estimates using short-term hub height data. Renewable Energy. 2010; 35(10):2340-2347.
15. Oluleye A and Ogungbenro SB. Estimating the wind energy potential over the coastal stations of Nigeria using power law and diabatic methods. African Journal of Environmental Science and Technology. 2011; 5(11):985-992.
16. Gualtieri G and Secci S. Comparing methods to calculate atmospheric stability-dependent wind speed profiles: a case study on coastal location. Renewable Energy. 2011b; 36(8):2189-2204.
17. Peña A, Gryning S-E, and Hasager CB. Measurements and modelling of the wind speed profile in the marine atmospheric boundary layer. Boundary-Layer Meteorology. 2008; 129(3):479-495.
18. Newman JF and Klein PM. The impacts of atmospheric stability on the accuracy of wind speed extrapolation methods. Resources. 2014; 3(1):81-105.
19. Gualtieri G. Atmospheric stability varying wind shear coefficients to improve wind resource extrapolation: a temporal analysis. Renewable Energy. 2016; 87: 376–390.
20. Okorie ME, Inambao F, and Chiguvare Z. Evaluation of wind shear coefficients, surface roughness and energy yields over inland locations in Namibia. Procedia Manufacturing. 2017; 7:630–638.
21. Tenneekes A. The logarithmic wind profile. Journal of the Atmospheric Sciences. 1973; 30(2):234-238.
22. Schwartz M and Elliott D. Towards a wind energy climatology at advanced turbine hub-heights. in Proceedings of 15th Conference on Applied Climatology, Savannah, GA, USA, 2005.
23. Poje D and Cividini B. Assessment of wind energy potential in Croatia. Solar Energy. 1988; 41(6):543-554.
24. Mathos KP, Donnou HEV, Kouchadé CA, Kounouhewa BB. Vertical Extrapolation of Wind Speeds Under a Neutral Atmosphere and Evaluation of the Wind Energy Potential on Different Sites in Guinea. American Journal of Energy Engineering. 2020; 8(1): 9-17.
25. Hellman G. Uber die bewegung der luft in den untersten schichten der atmosphere," Meteorologische Zeitschrift, 1916; 34 :273-285.
26. Gualtieri G and Secci S. Wind shear coefficients, roughness, length and energy yield over coastal locations in Southern Italy. Renewable Energy. 2011a ; 36(3) :1081-1094.
27. Kulkarni S and Huang H.-P. Changes in surface wind speed over North America from CMIP5 model projections and implications for wind energy. Advances in Meteorology. 2014 ; 1-10.
28. van den Berg GP. Wind turbine power and sound in relation to atmospheric stability. Wind Energy. 2008 ; 11(2) :151-169.
29. Zoumakis NM. Dependence of the wind profile power law exponent on the Pasquill stability classes and height interval in a stably stratified surface boundary layer. Il Nuovo Cimento C. 1993 ;16(1) :79-81.
30. Weber R. Estimators for the standard deviations of lateral, longitudinal and vertical wind components. Atmospheric Environment. 1998 ; 32(21) :3639–3646.
31. Sucevic N, Djurisic Z. Vertical wind speed profiles estimation recognizing atmospheric stability. EEEIC, Conference Proceedings, Rome, Italy. 2011
32. Monin AS and Obukhov AM. Basic laws of turbulent mixing in the ground layer of the atmosphere. Proceedings of Geophysics Institute, National Academy of Science. 1954; 151:163-187.
33. Paulson CA. The mathematical representation of wind speed and temperature profiles in the unstable atmospheric surface layer. Journal of Applied Meteorology. 1970; 9(6):857-861.

34. Businger JA, Wyngaard JC, Izumi Y, and Bradley EF. Flux-profile relationships in the atmospheric surface layer. Journal of the Atmospheric Sciences. 1971; 28(2): 181-189.
35. Panosfky HA, Dutton JA. Atmospheric turbulence. New York: Wiley-Inter-science; 1983
36. Nelder A and Mead R. Simplex method for function minimization. Computer Journal. 1965 ; 7 :308-313.
37. Lagarias JC, Reeds JA, Wright MH and Wright PE. Convergence properties of the nelder-mead simplex method in low dimensions. SIAM Journal of Optimization. 1998 ; 9(1) :112-147.
38. Spera DA, and Richards TR. Modified power law equations for vertical wind profiles. In: Conference and workshop on wind energy characteristics and wind energy siting. Portland, OR, USA. 1979.
39. Akpinar S and Akpinar EK. Wind energy analysis based on maximum entropy principle (MEP)-type distribution function. Energy Conversion and Management. 2007 ; 48(4) :1140-1149.
40. Ben Amar F, Elamouri M, and Dhifaoui R. Energy assessment of the first wind farm section of Sidi Daoud, Tunisia. Renewable Energy. 2008 ; 33(10) :2311-2321.
41. Giannakopoulou E-M and Nhili R. WRF model methodology for offshore wind energy applications. Advances in Meteorology. 2014 ; 2014 :1-14.
42. Chai T and Draxler RR. Root mean square error (RMSE) or mean absolute error (MAE)? Arguments against avoiding RMSE in the literature. Geoscientific Model Development. 2014; 7(3) :1247-1250.
43. Fagbenle RO, Katende J, Ajayi OO and Okeniyi JO. Assessment of wind energy potential of two sites in North-East, Nigeria. Renewable Energy. 2011; 36(4):1277-1283
44. Carta JA, Ramirez P and Velazquez S. A review of wind speed probability distributions used in wind energy analysis: Case studies in the Canary Islands: case studies in the Canary Islands. Renew Sustain Energy Rev. 2009; 13(5):933-955.
45. Akpinar EK and Akpinar S. An assessment on seasonal analysis of wind energy characteristics and wind turbine characteristics. Energy Convers Manage. 2005; 46(11):1848-1867.
46. Akinsanola AA. Ogunjobi KO, Abolude AT, Sarris SC, and Ladipo KO. Assessment of Wind Energy Potential for Small Communities in South-South Nigeria: Case Study of Koluama, Bayelsa State. J Fundam Renewable Energy Appl. 2017; 7(2):1-6.
47. Fadare DA. A statistical analysis of wind energy potential in Ibadan, Nigeria, based on Weibull distribution function. Pac J Sci Technol. 2008; 9(1):110-119.
48. Ahmed AS. Wind Energy as a Potential Generation Source at Ras Benas, Egypt. Renewable and Sustainable Energy Reviews. 2010; 14(8):2167-2173.
49. Weisser D. A wind energy analysis of Grenada: an estimation using the Weibull density function. Renewable Energy. 2003; 28(11):1803-1812.
50. Justus CG, Hargraves WR, Mikhail A. and Graber D. Methods for estimating wind speed frequency distributions. Journal of Applied Meteorology. 1978; 17(3):350-353.
51. Didane DH, Rosly N, Zulkafli MF and Shamsudin SS. Evaluation of Wind Energy Potential as a Power Generation Source in Chad. International Journal of Rotating Machinery. 2017; 1-10.
52. Donnou HEV, Akpo AB, Nonfodji GF and Kounouhewa BB. Variability of Onshore Wind Energy Potential in the 60 m above the Ground under Convective Atmosphere in Southern Benin. American Journal of Energy Research. 7(1):19-30.

53. Ajayi OO, Fagbenle RO, Katende J, Ndambuki JM, Omole DO and Badejo AA. Wind Energy Study and Energy Cost of Wind Electricity Generation in Nigeria: Past and Recent Results and a Case Study for South West Nigeria. Energies. 2014; 7:8508-8534.
54. Djossou J, Akpo AB, Affèwé JD, Donnou HEV, Liousse C, Léon J, Nonfodji FG and Awanou CN. Dynamics of the inter tropical front and rainy season onset in benin. Current Journal of Applied Science and Technology,2017 ; 24(2) :1-15.
55. Jarmalavicius D, Satkunas J, Zilinskas G, and Pupienis D. The influence of coastal morphology on wind dynamics. Estonian Journal of Earth Sciences. 2012 ; 61(2) :120-130.
56. Peña A and Gryning SE. Charnock's roughness length model and non-dimensional wind profiles over the sea. Boundary-Layer Meteorology. 2008 ; 128(2) :191-203.
57. Chang Y, Tan J, Grimmond S, and Tang Y. Distribution of aerodynamic roughness based on land cover and DEM—a case study in shanghai, China. in *Proceedings of* ICUC9-9th International Conference on Urban Climate Jointly with 12th Symposium on the Urban Environment, Toulouse, France, 2015
58. Boro D, Donnou HEV, Kossi I, Bado N, Kieno FP and Bathiebo J. Vertical Profile of Wind Speed in the Atmospheric Boundary Layer and Assessment of Wind Resource on the Bobo Dioulasso Site in Burkina Faso. Smart Grid and Renewable Energy. 2019 ; 10 :257-278.
59. Yahaya S, Frangi JP, and Richard DC. Turbulent characteristics of a semiarid atmospheric surface layer from cup anemometers-effects of soil tillage treatment (Northern Spain). Annales Geophysicae. 2003 ; 21(10) :2119-2131.
60. Fritz BK, Hoffmann WC, Lan Y, Jhomson S, and Huan Y. Low-level atmospheric temperature inversions and atmospheric stability: characteristics and impacts on agricultural applications. Agricultural Engineering International. CIGR Journal Ejournal PM. 2008 ; 10.
61. Salami AA, Ajavon ASA, Kodjo MK and Bédja K. Evaluation of wind Potential for an Optimum Choice of Wind Turbine Generator on the sites of Lomé, Accra and Cotonou Located in the Gulf of Guinea. Int. Journal of Renewable Energy Development. 2016 ; 5(3) :211-233.
62. Ouldbilal B, Ndongo M, Sambou V, Ndiaye PA and Kebe CM. Diurnal characteristics of the wind potential along the northwestern coast of Senegal. International Journal of the Physical Sciences. 2011 ; 6(35) :7950-7960.
63. Ouldbilal B, Ndongo M, Kebe CMF, Sambou V and Ndiaye PA. Feasibility study of wind energy potential for electricity genaration in the northwestern coast of Senegal. Energy Procedia. 2013 ; 36 :1119-1129.
64. Adaramola MS, Agelin-Chaab M, Paul SS. Assessment of wind power generation along the coast of Ghana. Energy Conversion and Management. 2014 ; 77 :61-69.
65. Na U, Oluleye A and Ka I. Investigation of Wind Power Potential over Some Selected Coastal Cities in Nigeria. Innovative Energy & Research. 2017 ; 6(1) :1-12.
66. Youm I, Sarr J, Sall M, Ndiaye A and Kane MM. Analysis of wind data and wind energy potential along the northern coast of Senegal. Rev. Energ. Ren. 2005 ; 8(2) : 95-108.
67. Mikhail AS. and Justus CG. Comparison of Height Extrapolation Models and Sensitivity Analysis. Wind Engineering. 1981; 5(2)
68. Ajavon ASA, Salami AA, Kodjo MK, Bédja K. Comparative characterization study of the variability of wind energy potential by wind direction sectors for three coastal

sites in Lomé, Accra and Cotonou. Journal of Power Technologies. 2015 ; 95(2) : 134-142